NATIONAL BUREAU OF STANDARDS REPORT

8561

PROCEDURES FOR PRECISE DETERMINATION OF THERMAL RADIATION PROPERTIES

to

Research and Technology Division
United States Air Force
Wright-Patterson Air Force Base, Ohio

U.S. DEPARTMENT OF COMMERCE
NATIONAL BUREAU OF STANDARDS

THE NATIONAL BUREAU OF STANDARDS

The National Bureau of Standards is a principal focal point in the Federal Government for assuring maximum application of the physical and engineering sciences to the advancement of technology in industry and commerce. Its responsibilities include development and maintenance of the national standards of measurement, and the provisions of means for making measurements consistent with those standards; determination of physical constants and properties of materials; development of methods for testing materials, mechanisms, and structures, and making such tests as may be necessary, particularly for government agencies; cooperation in the establishment of standard practices for incorporation in codes and specifications; advisory service to government agencies on scientific and technical problems; invention and development of devices to serve special needs of the Government; assistance to industry, business, and consumers in the development and acceptance of commercial standards and simplified trade practice recommendations; administration of programs in cooperation with United States business groups and standards organizations for the development of international standards of practice; and maintenance of a clearinghouse for the collection and dissemination of scientific, technical, and engineering information. The scope of the Bureau's activities is suggested in the following listing of its four Institutes and their organizational units.

Institute for Basic Standards. Electricity. Metrology. Heat. Radiation Physics. Mechanics. Applied Mathematics. Atomic Physics. Physical Chemistry. Laboratory Astrophysics.* Radio Standards Laboratory: Radio Standards Physics; Radio Standards Engineering.** Office of Standard Reference Data.

Institute for Materials Research. Analytical Chemistry. Polymers. Metallurgy. Inorganic Materials. Reactor Radiations. Cryogenics.** Office of Standard Reference Materials.

Central Radio Propagation Laboratory.** Ionosphere Research and Propagation. Troposphere and Space Telecommunications. Radio Systems. Upper Atmosphere and Space Physics.

Institute for Applied Technology. Textiles and Apparel Technology Center. Building Research. Industrial Equipment. Information Technology. Performance Test Development. Instrumentation. Transport Systems. Office of Technical Services. Office of Weights and Measures. Office of Engineering Standards. Office of Industrial Services.

---

* NBS Group, Joint Institute for Laboratory Astrophysics at the University of Colorado.
** Located at Boulder, Colorado.

NATIONAL BUREAU OF STANDARDS REPORT

NBS PROJECT

42108-11-4210481

NBS REPORT

8561

PROCEDURES FOR PRECISE DETERMINATION
OF THERMAL RADIATION PROPERTIES

PROGRESS REPORT No. 23

May 1, 1964 - July 31, 1964

Contract No. DO(33-615) 64-1005
Task No. 738103

Research and Technology Division
United States Air Force
Wright-Patterson Air Force Base, Ohio

U.S. DEPARTMENT OF COMMERCE

NATIONAL BUREAU OF STANDARDS

1. SUMMARY

The integrating sphere of the laser reflectometer was coated with 3M Velvet white paint, and preliminary measurements were made at room temperature of the reflectance of two types of shallow cavities with several different depth-to-radius ratios. Fair agreement with theory was obtained even without making corrections for known errors. A lock-in amplifier system was procured for use with the laser reflectometer. A heater was constructed for operation to 800°K.

The angular sensitivity of the thermopile detector used with the ellipsoidal reflectometer was evaluated and found not to be a problem. Several different integrating devices were designed and constructed in an effort to overcome the errors due to the variation in spatial sensitivity of the detector.

The theoretical relationships between electrical resistivity and emissivity of metals were reviewed, and curves are presented showing the agreement of the theoretical curves and experimental data obtained on the platinum and platinum-13% rhodium working standards of normal spectral emittance. The data obtained on these alloys and on oxidized Inconel are compared to data on the same materials reported in the literature.

Two procedures for measurement of normal spectral emittance in the 15 to 32.4 micron range were evaluated. One of the procedures was found to give better precision and accuracy than the other. The emittance of a platinum working standard of emittance was measured out to 32.4 microns. New specimens of platinum-13% rhodium alloy, Kanthal and Inconel have been procured on Bureau funds and cut to size for use as working standards of normal spectral emittance.

2. INTEGRATING SPHERE REFLECTOMETER

2.1 Background

Spectral emittance measurements obtained by direct comparison of the spectral radiant flux density of a hot specimen to that of a laboratory blackbody furnace at the same temperature are subject to large errors not only at wavelengths that are appreciably shorter than the peak of the Planck distribution function at the test temperature but also at temperatures above those at which standard thermocouples can be used.

The errors at the short wavelengths arise from two sources: 1) The energy available for measurement decreases rapidly with decreasing wavelength at wavelengths below the peak, hence there is not enough energy to permit measurements of the highest accuracy at the shortest wavelengths. 2) The temperature dependance of spectral flux density increases rapidly with decreasing wavelength at wavelengths below the peak; therefore, a small temperature difference between specimen and blackbody reference will cause a much larger error in emittance at wavelengths shorter than the peak than at wavelengths longer than the peak.

At temperatures above those at which standard thermocouples can be used, the temperature scale is based upon the optical pyrometer, and either an optical pyrometer or a radiation pyrometer is commonly used for temperature measurements in this range. These instruments are accurate for measuring the temperature of a laboratory blackbody furnace and they also measure the brightness temperature or the radiance temperature of a specimen with acceptable accuracy. Conversion of this brightness or radiance temperature to true temperature, however, requires knowledge of the spectral emittance of the specimen over the appropriate wavelength range. Thus one is faced with the necessity of knowing the emittance in order to measure the temperature, which is in turn required to evaluate the emittance.

Reflected flux, as contrasted to emitted flux, is nearly independent of the temperature of the specimen, at least over temperature intervals that do not exceed about 50°K. For opaque specimens, the emittance is equal to one minus the reflectance, by Kirchhoff's law. The measurement of reflectance involves only the comparison of incident and reflected flux. Thus, such measurements would appear to offer the possibility of considerably increasing the precision with which emittance can be determined, particularly in the short wavelength and high temperature regions where direct measurements are subject to large errors. However, for reflectance to be equal to one minus the normal spectral emittance, the reflectance must be measured under conditions of either normal illumination and hemispherical viewing, or diffuse illumination and normal viewing.

Three general methods have been used to measure reflectance under these conditions: (1) the integrating sphere, (2) the integrating hemisphere, and (3) the hemispherical source instruments. The integrating sphere is generally preferred and is the most widely used at wavelengths for which suitable sphere coatings are available. The principal problem in measuring reflectance of a specimen at high temperatures is to distinguish between the flux reflected by the specimen and that emitted by the hot specimen. This can be done by chopping the beam of incident flux, so that an ac signal is produced by the detector, which is synchronously amplified and recorded. The dc signal from the flux emitted by the hot specimen is not amplified, and appears only as noise. The signal-to-noise ratio can be increased by using a source having a high flux density within the wavelength interval of interest. A helium-neon continuous wave laser was selected for this purpose because its flux density within the narrow wavelength band at which it lases is several orders of magnitude larger than the flux emitted by any solid specimen at a temperature below its melting point, within the same wavelength interval.

Design and construction of the integrating-sphere reflectometer with a helium-neon laser source was described in a previous report.

2.2 Description of Integrating Sphere Reflectometer

a. Basic Design. A cross sectional view of the integrating sphere is shown in Fig. 1. The sphere coating used for the preliminary measurements was a white primer with a thin top coat of 3M Velvet paint.[1/]

1/ The primer was DuPont 65-3010 white, sprayed to a thickness of about 0.003 in. and air dried.

The reflectance of the sphere coating relative to MgO is shown in Fig. 2. Preliminary goniophotometric measurements indicate that the coating is a good approximation of a perfect diffuser.

The laser beam is nearly parallel, and is about 1/4 inch in diameter at the specimen port. It strikes the specimen at an angle of 6° to the normal.

b. Heater design. A heater, for heating specimens 1/2 inch in diameter to temperatures up to 800°K, has been built. A schematic drawing of this heater is shown in Fig. 3. An important design feature is the provision of holders for specimens of thickness of 1/4 inch for nonmetallic materials and 0.065 inch for metals.

c. Detection System. A new detection system consisting of a lock-in amplifier, preamplifier, and lead sulfide cell has been designed. The amplifier and detector have been procured, and the preamplifier is being constructed in the NBS Electronic Instrumentation Section.

2.3 Theory of the Integrating Sphere

The theory of the integrating sphere reflectometer for a perfectly diffuse sphere wall and diffusely reflecting specimens has been presented by Jacquez and Kuppenheim.[2/] For measurements by the substitution method (in which first the standard and then the specimen is placed over the specimen port and measured) the reflectance of the specimen, ρ_s, relative to the reflectance of the standard ρ_{st}, is expressed by

$$\frac{B_s}{B_{st}} = \frac{\rho_s}{\rho_{st}} \left[1 - \frac{(\rho_{st} - \rho_s)\, c/S}{1 - \rho^{\,d}/S - \rho^{\,c}/S} \right] = E \frac{\rho_s}{\rho_{st}} \qquad (1)$$

where

B_s = brightness at detector port with specimen at specimen port.

B_{st} = brightness at detector port with standard at specimen port.

ρ = reflectance of sphere wall, 0.825 at .632 microns

a = spherical area of entrance port, 0.994 in.^{2}

b = spherical area of detector port, 0.442 in.^{2}

c = spherical area of specimen port, 1.227 in.^{2} [3/]

S = total area of sphere wall, $4\pi R^2$, 615.752 in.^{2}

d = S - a - b - c, total reflecting area of sphere wall -613.089 in.^{2}

2/ Jacquez, John A., and Kuppenheim, Hans F., Theory of the Integrating Sphere, Jour. Optical Soc. of America, 45, pp 460-470 (1955).

3/ Computed for shallow cavity tests described later.

The ratio B_s/B_{st} is the ratio of the reflectometer readings for the specimen and standard, respectively, and E is the correction factor for flux losses through the sphere ports. Substituting the values given in the table above for the sphere shown in Fig. 1, we get

$$E = \frac{.1786 - 0.00199\ \rho_{st}}{.1786 - 0.00199\ \rho_s} \simeq 1.00 \qquad (2)$$

For reasonable values of ρ_s and ρ_{st}, the factor E varies from 1.00 by less than 1%. Hence this correction will be neglected in the preliminary checking of the reflectometer.

The theory developed above is for the "perfect sphere", where the specimen and standard have a spherical surface of the same radius as the sphere. It can be modified for the case of flat specimens. No theory is available for the case of specularly reflecting specimens.

Integrating sphere reflectometers can also be operated by the comparison method in which there is both a standard port and a specimen port. In this case, both standard and specimen are always in position, but they are illuminated alternately.

2.4 Calibration of Integrating Sphere

Theory. A calibration procedure has been developed, based on previous studies of Kelly and Moore[4/]. In this study the Gouffé equation relating the "emittance" of a shallow cavity to its geometry and the emittance of its walls was verified experimentally, by measuring with a General Electric recording spectrophotometer, the reflectance of shallow cavities of known properties. Two types of cavities were used. The first was constructed so that only the light reflected from the bottom of the cavity was permitted to leave the opening. A sketch of this cavity is shown in Fig. 4. The depth of the cavity was adjustable to give L/R ratios from 0 to 2.0. (L is depth and R is radius of the cavity opening.) If the bottom of the cavity is a perfect diffuser, the fraction, f, of the energy escaping through the opening is

$$f = \frac{1}{1 + \left(\frac{L}{R}\right)^2} \qquad (3)$$

Equation 3 is based on the assumption that the cross-sectional area of the incident beam is small compared to the area of the bottom of the cavity, and strikes the bottom at its center. Such illumination is referred to as center point illumination. The theory can be modified to accommodate other conditions of illumination, as is described in the fererence.

The second type of cavity had diffusely reflecting walls and bottom, as is illustrated in Fig. 4. The experimental data agreed well with that computed from the Gouffé equation for the reflectance of the cavity, ρ_c, in terms of the L/R ratio and the reflectance of the cavity walls, ρ_w:

4/ Kelly, F.J. and Moore, D.G., A Test of Analytical Expressions for the Thermal Emittance of Shallow Cylindrical Cavities. Symposium on Thermal Radiation of Solids, San Francisco, Cal., March 1964.

$$\rho_c = 1 - \frac{(1-\rho_w)[1+\rho_w(\frac{a}{A} - f)]}{1-\rho_w(1 - \frac{a}{A})} \qquad (4)$$

where $\frac{a}{A} = \frac{1}{2(1+\frac{L}{R})}$ and $f = \frac{1}{1+(\frac{L}{R})^2}$

($\frac{a}{A}$ is the ratio of the area of the opening to the total area of the cavity, opening included, and f is the fraction of the incident flux leaving the cavity on the first reflection.)

Eq. 4, like eq. 3, is based on center point illumination, and the assumption that the walls and bottom of the cavity are perfectly diffuse reflectors. A plot of the reflectance ratio, ρ_c/ρ_w, as a function of the $\frac{L}{R}$ ratio computed by eq. 4 is shown in Fig. 5, for different values of ρ_w.

The shallow cavity tests are particularly suitable for calibration of the integrating sphere reflectometer for two reasons: (1) the Gouffé equations have been verified experimentally with an instrument of proven reliability, and (2) the geometric distribution of the flux reflected from the velvet-lined cavity (Fig.4a) varies from that of a perfectly diffusing reflector in that at an L/R ratio of 2.0 practically no flux is reflected at angles greater than about 30° to the normal.

b. Experimental. Preliminary measurements were made at the reflectance of the two shallow cavities. In each case the bottom of the cavity (L/R = 0) was used as the standard, and the L/R ratio was varied up to 2.0.

All measurements were made with the laser operating at 0.632μ, and the incident beam of approximately ¼ inch diameter was centered on the bottom of the cavity at the L/R = 0 position. Thus the incident beam approximated center point illumination.

The detector was mounted in the viewing port as is shown in Fig. 6. According to theory, the detector should measure the flux density of an area on the sphere wall. When the flashed opal glass covered the detector port, the detector viewed the glass, and hence measured the flux density at the detector port. When the opal glass was removed and a black sleeve inserted into the detector port, the detector viewed an area on the sphere wall diametrically opposite the detector port, and hence measured the flux density of that area.

Preliminary measurements of the ρ_c/ρ_w ratio for the first reflection cavity are plotted as a function of L/R ratio in Fig. 7. Similar data for the lined cavity are shown in Fig. 8. In both figures the solid line represents the ρ_c/ρ_w ratio computed from the appropriate Gouffé equation for the cavity lining of reflectance of 0.825 at 0.632μ, as reported by Kelly and Moore.

No attempt has been made as yet to correct the measured values for known errors. These include (1) deviations from center point illumination (2) loss of flux through sphere ports, and (3) flux from the first reflection that is incident on the detector. Rigorous computation of the correction is possible for (1) and (2) but for (3) a correction cannot be made without complete information on the geometric distribution of the flux reflected from the specimen on the first reflection. Before obtaining such information, attempts will first be made to eliminate this error by internal baffling in the sphere.

2.5 Future Plans

Work with the integrating sphere reflectometer during the next quarter will be concentrated along the following lines:

a. Calibration. Complete the shallow cavity calibration at 0.632 and 1.15 microns with the present sphere coating. Coat the sphere with barium sulfate and repeat calibrations at 0.632 and 1.15 microns, and calibrate at 3.39 microns.

b. Measurements. Begin comparative reflectance measurements at 0.632 and 1.15 microns at temperatures up to 800°K.

c. Theoretical studies.

(1) Make necessary corrections to the shallow cavity calibration, and/or modify the sphere design as necessary to reduce or eliminate known errors.

(2) Study use of an "appended sphere (instead of the shallow cavity) for absolute reflectance measurements.

III. ELLIPSOIDAL MIRROR REFLECTOMETER

3.1 Background

In the ellipsoidal mirror reflectometer a Perkin-Elmer model 83 monochromator supplies a beam of chopped monochromatic flux, which is directed to a large spherical mirror, which in turn focuses the beam through a small hole in the ellipsoidal mirror onto the specimen at the first focus of the ellipsoid. The axial ray of the incident beam strikes the specimen at an angle of about 7° to the normal. The ellipsoidal mirror collects the flux reflected from the specimen and focuses it onto the detector at the second focus of the ellipsoid. The detector can be positioned alternately at the first or second focus, to measure the incident or reflected flux. The ellipsoidal mirror has a magnification factor of about 5. For this reason, a large area detector must be used.

A Golay cell detector having a sensitive area one centimeter in diameter was used in the earlier work with the reflectometer. While it had the desired sensitivity it was also highly microphonic, particularly when used with its sensitive area in a horizontal position, as is the case with this equipment. Extensive attempts to isolate the detector from building vibrations by use of a seismic table mount, and from air-borne noise by acoustic insulation of the reflectometer enclosure, were not effective in reducing the noise to a reasonable level. Use of the Golay cell detector was abandoned as a result of these experiments.

As a substitute detector a sensitive thermopile, having a sensitive area of one square centimeter, was procured. It was found to be essentially free from microphonics, but tests indicated that it varied significantly in sensitivity over its sensitive area. The sensitive area was made up of ten very thin black-coated plates, each 2 x 5 mm in size. These plates were arranged in two columns of five rows to produce the one square centimeter sensitive area. One thermocouple was attached to each plate. When a fine-line image about 12 mm long was moved across the sensitive area in a direction parallel to the rows, two peaks in sensitivity were observed, roughly corresponding to the centers of the two columns of plates. When the image was moved in a direction parallel to the columns, five peaks were observed, roughly corresponding to the centers of the five rows of plates.

3.2 Angular Sensitivity of Detector

Since the detector needed to be equally sensitive to radiation striking at any solid angle from 0 to 24°, the angular sensitivity of the thermocouple detector was measured. To make this measurement the detector was mounted on a milling head with its sensitive area in a vertical plane and with the two columns of plates vertical, in a position such that the center line of the sensitive area coincided with the vertical axis of rotation of the milling head. An image of the exit slit of the monochromator, 3 x 3 mm in size, was focused on the center of the sensitive area from a direction normal to it, by means of a 6-in. diameter spherical mirror having a 49-in. radius of curvature. The cone of rays thus had a half-angle width of about 3½°. The monochromator was adjusted to give a band of flux centered at 2.2 microns. The response of the detector was recorded as R_n when the axial ray of the incident beam was normal to the sensitive area. The milling head was then rotated to give incident angles of 5, 10, 15, 20, 25, 30, 40, 50, 60 and 70° to the normal, and the response of the detector was recorded at each setting as R_θ, θ being the angle of incidence. The data were normalized by dividing each reading by the reading at normal incidence, and plotted as a function of angle of incidence to produce the curve shown in Fig. 9. Similar measurements were made with a cover plate 0.15 in. in thickness with a 1 x 1 cm hole centered over the sensitive area. The entire procedure was then repeated with flux of 8 microns wavelength.

The experimental curves are compared in Fig. 9 with two computed theoretical curves. The top curve, in which $R_n/R_\theta = 1$ at all angles would be obtained if the detector was equally sensitive to flux striking it at all angles, and if all of the incident flux struck the sensitive area. The lower curve, in which $R_n/R_\theta = \cos\theta$, would be obtained if the detector was equally sensitive to flux striking it at all angles, and was completely filled at normal incidence.

From the experimental curves in Fig. 9 it can be seen that the sensitivity increases slightly from normal to 20°, then decreases. The increase is undoubtedly due to the fact that as the illuminated area of the detector increases, the more sensitive areas, as shown in the previous report, become illuminated. The sharp drop in response beginning at about 30° is due to some of the flux being lost, either not admitted through the window or not striking the sensitive area if admitted. The presence of the cover plate increases the rate of fall off in this range, as might be expected.

Similar tests were made with the detector mounted with the five rows of plates vertical. The results shown in Fig. 10 are similar to those in Fig. 9 except that the increase in signal from 0 to 20° was not observed. This is undoubtedly due to the fact that as the angle was increased, more plates were illuminated, but in the same relative areas, hence the signal remained constant.

The curves plotted in Figs. 9 and 10 show no significant differences for flux of 2.2 and 8 microns, respectively. The fact that the curves are nearly flat from 0 to 25° indicates that variation in angular sensitivity will be no problem with the ellipsoidal reflectometer since with the present instrument the marginal rays strike the detector at an angle of approximately 24°.

3.3 Integrating Devices

The information on angular sensitivity in Section 3.2 above and the data on spatial sensitivity in the previous report indicate the need for an integrating device to spread the incident flux uniformly over the detector sensitive area regardless of the image size or uniformity, or the angular distribution of incident flux.

Results with a two-inch diameter integrating sphere coated with 3M Velvet white paint were given in the previous report. The major problem with this approach is the sphere wall coating. Date are presented in Fig. 11, showing sphere efficiency as a function of reflectance of the sphere wall for spheres of 1, 2, and 3 in. diameters. The curves were computed from equations given by Jacquez and Kuppenheim[2]. These curves indicate that, for high efficiency, high diffuse reflectance of sphere wall and small diameter of sphere are required. High sphere efficiency is essential at the longer wavelengths where only a small amount of incident flux is available with the particular monochromator that is being used.

White paints in general have very low reflectance at wavelengths beyond about three microns; hence painted spheres are not suitable for use at long wavelengths. Polished metal surfaces, on the other hand, have high reflectance at wavelengths from the visible into the far infrared. They are not normally considered suitable for use in integrating spheres because they reflect specularly. However, since a suitably contoured metal surface might provide reasonably good diffusing power, a specially contoured surface was prepared for trial. The surface consisted of a series of spherical depressions, of 1/16 in. radius, spaced 0.088 in. on centers in a hexagonal close pack array. Goniophotometric reflectance curves for this surface with white light are shown for 45° illumination in Fig. 12, and for normal illumination in Fig. 13.

Footnote 2, p. 3

While the surface is far from a perfect diffuser, it does reflect some energy in all possible directions, and thus it has promise for use in an integrating device.

3.4 Future Plans

Work during the next quarter will be along the following lines:

a. A satisfactory integrating device will be developed to overcome the effect of variations in spatial sensitivity of the thermocouple detector.

b. When a satisfactory diffuser-detector combination has been obtained, the ellipsoidal mirror reflectometer will be calibrated for use over the wavelength range of approximately 2 to 15 microns.

c. A theoretical study of the errors in the ellipsoidal mirror reflectometer will be initiated.

4. COMPARISON OF SPECTRAL EMITTANCE DATA FOR PLATINUM WORKING STANDARDS WITH VALUES PREDICTED BY THE HAGEN-RUBENS RELATION AND WITH LITERATURE VALUES

4.1 Background

One of the long range objectives of the thermal radiation work has been to obtain a better understanding of the mechanisms involved in the interaction between matter and electromagnetic radiation; the processes of reflection, absorption, transmission, and emission. Such an understanding can contribute appreciably not only to the development of methods for evaluating the thermal radiation properties of materials, but also to the design of equipment used in such measurements as well as to the evaluation of errors.

The work that has been done on theory will be summarized in the next annual summary report. As one of the last phases of this work, the data obtained earlier for the platinum and platinum-13% rhodium working standards were compared with values predicted by the so-called Hagen-Rubens[5/] equation (Drude-Zener). This equation relates normal spectral emissivity, $\epsilon_o(\lambda)$, to dc resistivity, ρ, and wavelength, λ

$$\epsilon_o(\lambda) = 0.365(\rho/\lambda)^{\frac{1}{2}} - 0.0464(\rho/\lambda) \qquad (1)$$

Equation 1 is applicable at long wavelengths and/or at high temperatures. It is derived from classical electromagnetic theory assuming a negligible phase change of the electric field caused by the interaction of the wave with the metal.

5/ Hagen, E. and Rubens, H., "Emissions-vermogen und electrische heitfahigkeit der Metallegrerungen," Verh. Deut. Phys. Ges. 6, 128 (1904).

4.2 Agreement of Spectral Data with Hagen-Rubens Equation

Fig. 14 shows the type of agreement observed for platinum. The solid lines represent the average measured emittances of the six platinum working standards. The vertical lines indicate the statistical uncertainty, expressed as the total standard deviation, due to error of measurement and difference in specimens. The two broken lines represent the values computed from equation (1), using resistivity data given by Caldwell.[6/]

There are some obvious areas of mismatch between the measured and computed values. The maximum near 9 microns at all three temperatures could be caused by (a) a bound electron phenomenon, (b) an instrumentation error, or (c) an impurity effect. No impurity was identified when a specimen was examined by electron diffraction, but further examinations are planned.

The rise in emittance values at wavelengths near 15 microns at the higher temperature is believed to be an instrumentation error. It has not been found in repeat measurements made on the same specimens after completing certain modifications in the spectrometer.

The maxima between 1 and 2 microns have previously been attributed to resonance of bound electrons, although data reported by Roberts[7/] indicate that no resonance effect is to be expected in this wavelength region. The maxima may be due to instrumentation error, since they occur in wavelength regions where the energy is low.

At 1100°K a reasonable fit of the experimental data at wavelengths beyond about 3.5 microns was obtained with the values computed from the resistivity of platinum at 800°K given by Caldwell[6/]. At 1400°K, however, a resistivity higher than that given by Caldwell was required to produce even an approximate fit, and at 800°K a resistivity lower than that given by Caldwell was required. These results indicate that equation (1) cannot be used with published resistivities to extrapolate the measured emittance data to temperatures above 1400°K or below 800°K. Information regarding the most suitable methods for extrapolation of the spectral emittance data to other temperatures and wavelengths will be included in the final summary report.

The properties of the platinum-13% rhodium alloy are similar to those of pure platinum. Normally the presence of an alloying constituent might be expected to introduce changes in the properties. However, these effects are minor and appear as a slight increase in emittance and also in resistivity, as compared to pure platinum. The experimental data are compared in Fig. 15 with values computed from equation (1). The agreement between computed and observed values is about as good as was the case for platinum. In general, however, application of the simplified theory to alloys should be done with caution since an alloy, in most cases, can no longer be considered as a simple metal.

6/ Caldwell, F.R. "Thermocouple Materials", NBS Monograph 40, March 1962.

7/ Roberts, S. "Interpretation of the Optical Properties of Metal Surfaces," Phys Rev 100, 1667 (1955).

The observed data show the maximum between 9 and 10 microns that was observed with platinum at each temperature, but the maximum between 1 and 2 microns appears only in the platinum-13% rhodium data at 800°K, and the rise in emittance at wavelengths near 15 microns was not observed with the alloy specimens.

4.3 Comparison of Standards Data with Literature Values

Since the optical properties of a metal are markedly affected by the conditions of the surface, differences in values reported by different investigators are to be expected. Recently the problem of surface characterization of metals[8] has received increasing attention. The complexity of the problem makes it extremely difficult to characterize completely a metal specimen so that data obtained in one laboratory can be reproduced on other specimens of the same material prepared and measured in a second laboratory. In spite of these difficulties, comparison of data obtained on the working standards of normal spectral emittance with data obtained in other laboratories on similar specimens may serve a useful purpose.

Fig. 16 shows values for normal spectral emittance of platinum at 1400°K obtained in three other laboratories, together with the data reported for the working standards. The agreement is reasonably good, except that the increase in emittance at 14 to 15 microns was not reported by other investigators.

Fig. 17 shows values for oxidized Inconel obtained in other laboratories together with the data on the working standards. In general, when oxidation times were equivalent, agreement is satisfactory.

A brief description of the measurements made in other laboratories is given in Table I.

5. NORMAL SPECTRAL EMITTANCE

5.1 Background

Equipment and procedures were developed earlier for measuring the normal spectral emittance, over the wavelength range of 1 to 15 microns, of metal specimens that can be heated by passing a current through them, as described in WADC TR 59-510 Pt IV. Recently the equipment was modified to operate in the 15-38 micron range by (1) enclosing it in an atmosphere of super-dry CO_2-free air, (2) replacing the thermocouple detector with a new high-sensitivity detector with a cesium iodide window, (3) replacing the sodium chloride prism with a cesium bromide prism, and (4) by addition of filters to reduce scattered light in the monochromator. Wavelength calibration of the spectrometer with the cesium bromide prism was completed.

8/ DeWitt, David P., "Surface Characterization of Real Metals," Symposium on Thermal Radiation of Solids, Session II Surface Effects ASD (USAF) NBS, NASA, San Francisco, March 1964.

Two test procedures were developed for use in the 15-38 micron range; (A) a black polyethylene filter was placed over the entrance slit to the monochromator, and the spectrometer controls were set to permit scanning from 12.4 to 38.5 microns, and (B) the range was subdivided into three overlapping portions, 12.4 to 27.3, 26.4 to 32.4, and 32.4 to 38.5 microns, respectively. The black polyethylene filter was used in the 12.4 - 27.3 micron portion, and the spectrometer controls were set to permit scanning over this range. In the two longer wavelength portions the black polyethylene filter was replaced with a CaF_2 reststrahlen plate, and the controls were set to permit scanning over the respective portions of the range.

5.2 Evaluation of Test Procedures

The test procedures were evaluated by using the combination of a 50% transmittance sector-disc attenuator and a laboratory blackbody furnace to simulate a specimen having a normal spectral emittance of 0.50 at all wavelengths. Four tests were made at each of the three temperatures 800, 1100 and 1300°K, using each of the two procedures. The data for the first two wavelength ranges were reduced at 23 wavelengths in the 12.4 to 26.8 micron range and 15 wavelengths in the 26.4 to 32.6 micron range. The average standard deviations are shown in Table II, and the overall average emittances are shown in Table III.

The data in Table II show that the overall scatter, measured as the average standard deviation at the 23 and 15 wavelengths, respectively, was smaller for procedure A than for procedure B in four of the six cases, and the data in Table III show that the accuracy was better for procedure A than for procedure B in all six cases. On the basis of these results, procedure A has been selected for use in future measurements in these wavelength ranges.

5.3 Measurements on Platinum

The normal spectral emittance of a platinum working standard of normal spectral emittance was measured over the wavelength ranges of 1 to 15 microns and 13 to 28.5 microns, at 1300°K. Three separate runs were made and the data were reduced as before. The average emittance values and standard deviations are plotted in Fig. 18. The curve for the average emittance values shows that the results with the sodium chloride prism (1 to 15μ) and those with the cesium bromide prism (12.8 to 28μ) check well within the known precision of measurement in the range where the two curves overlap. The data on the standard deviations of the measured values indicate that the precision of measurement is about the same in the two ranges.

The rise in emittance in the 13 to 15 micron region that was found in the original calibration was not confirmed in the most recent measurements with either prism.

5.4 New Working Standards

The new working standards of normal spectral emittance have been purchased on Bureau funds, and are being prepared prior to calibration.

TABLE I

BRIEF DESCRIPTION OF METHODS OF MEASUREMENT AND SAMPLE PREPARATION FOR CITED LITERATURE VALUES

Material	Authors	Method/Apparatus	Specimen Description
Platinum	Schatz and McCandless [1]	Double-beam recording spectrophotometer with transfer optics to view separate specimen and blackbody furnaces.	Commercial foil, no additional description given.
Platinum	Maki, Stair & Johnson [2]	Single-beam recording spectrophotometer with transfer optics and traveling optical bench to alternately view blackbody furnace and resistance heated specimen.	Commercial grade strip ($8\frac{1}{2} \times \frac{1}{4} \times \frac{1}{32}$"), annealed at 1525 K for one hour.
Oxidized Inconel	Maki, Stair & Johnson [2]	Same as above	Commercial Inconel strip, sandblasted and heated at elevated temperature for six hours.
Oxidized Inconel	Blau, et al [3]	Single-beam recording spectrophotometer with specimen imbedded in wall of hollow silicon carbide heating element with cavity to serve as blackbody.	No details given other than oxidized in air.
Platinum	Price [4]	Single-beam recording spectrophotometer with cylindrical specimens electrically heated in vacuum with lateral slit serving as blackbody.	Commercial 99.8% purity sheet.
Oxidized Inconel	Slemp & Wade [5]	Single-beam recording spectrophotometer views specimen as it rotates past viewing port of blackbody cavity furnace.	Oxidized in air for 20 minutes.

[1] Schatz, Elihu A. and McCandless, Lee C., "Research for High Emittance Coatings," Tech. Doc. Rept. No. ASD TR 62-443, Directorate of Materials & Processes, ASD, A.F. Systems Command, WPAFBase, Ohio, May 1962.

TABLE I- cont'd.

[2] Maki, Arthur G., Stair, Ralph and Johnston, Russell G., "Apparatus for the Measurement of the Normal Spectral Emissivity in the Infrared," J. of Res. NBS 64C, 99-102 (1960).

[3] Blau, Henry H. Jr., Marsh, John B., Martin, William S., Jasperse, John R., and Chaffee, Eleanor, "Infrared Spectral Emittance Properties of Solid Materials," Final Rept. AFCRL-TR-60-416, Geophysics Research Directorate of the Air Force Research Division, Cambridge, Mass., Oct. 1960.

[4] Price, Derek J., "The Emissivity of Hot Metals in the Infrared," Proc. Phy. Soc. (London) 59, 118 (1947).

[5] Slemp, Wayne S. and Wade, William R., "A Method for Measuring the Spectral Normal Emittance in Air of a Variety of Materials Having Stable Emittance Characteristics," Proceedings of Symposium on Measurement of Thermal Radiation Properties of Solids, Joseph C. Richmond, Editor, Page 443, NASA SP-31,(1963).

TABLE II

TABLE OF AVERAGE STANDARD DEVIATIONS

Temperature	Wavelength Range			
	12.40 - 27.30(μ) Procedure		26.40 - 32.40μ Procedure	
	A	B	A	B
800°K	0.398	0.522	0.346	0.220
1100°K	0.360	0.299	0.274	0.800
1300°K	0.342	0.447	0.338	0.436

TABLE III

TABLE OF AVERAGE MEASUREMENTS

Temperature	Wavelength Range			
	12.40 - 27.30(μ) Procedure		26.40 - 32.40(μ) Procedure	
	A	B	A	B
800°K	52.00	52.20	51.99	52.43
1100°K	50.53	51.77	50.52	53.21
1300°K	50.11	50.66	50.58	51.17

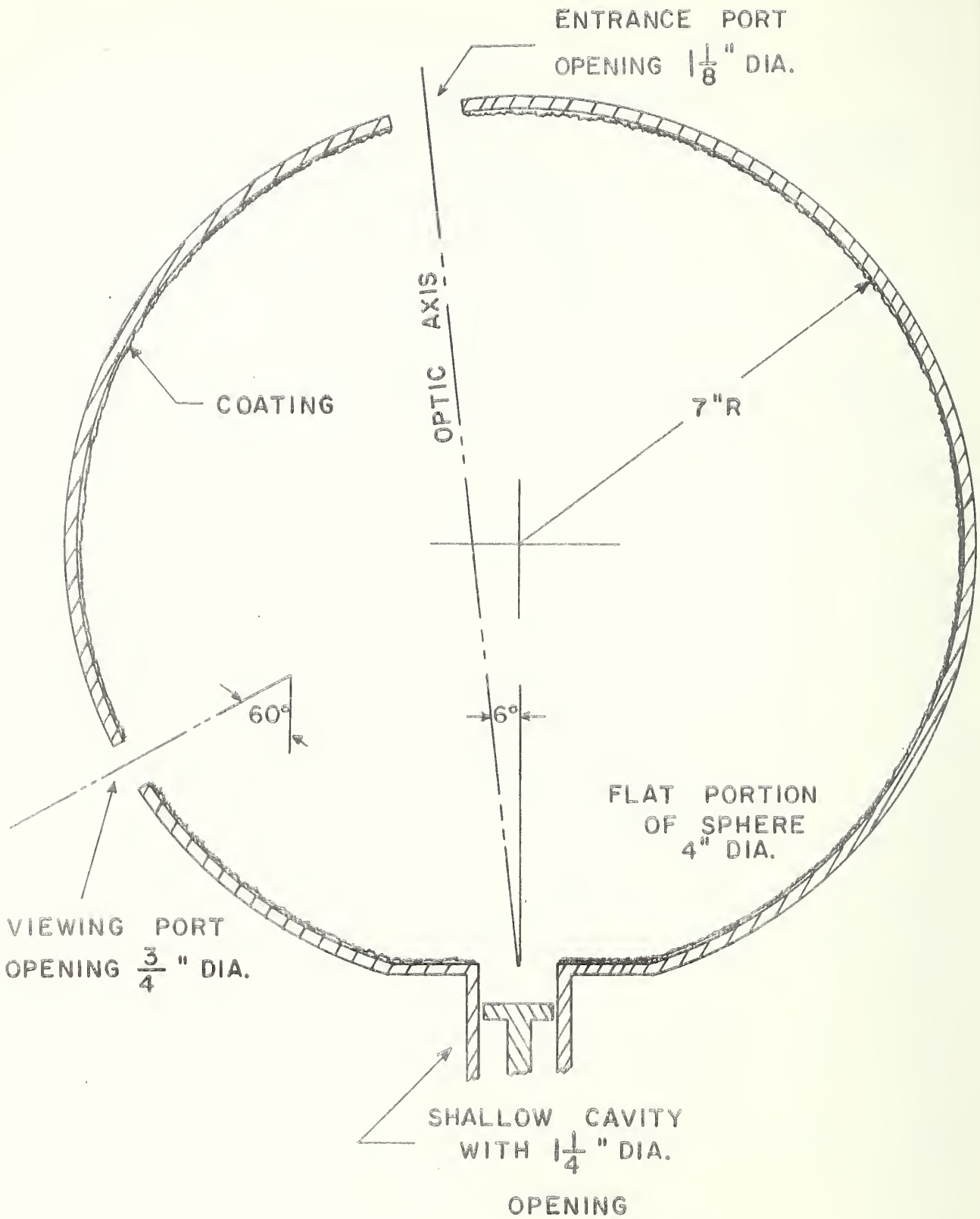

Figure 1. Significant dimensions and location of ports for 14-inch integrating sphere.

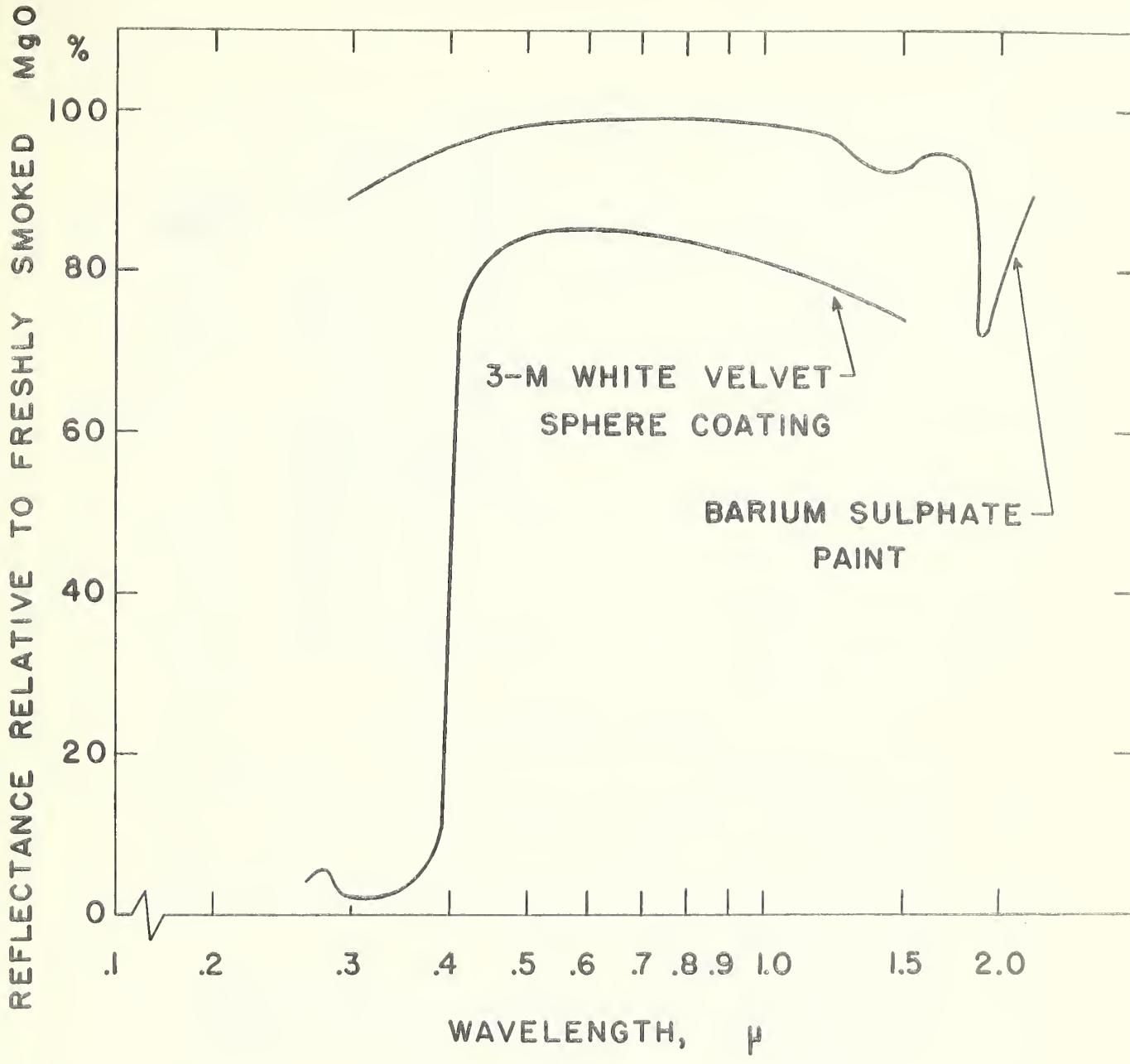

Figure 2. Spectral reflectance, relative to MgO, of the 3M white Velvet coating used on the integrating sphere, and of a $BaSO_4$ coating as reported by Middleton and Sanders, Illiminating Engineering 48, 254 (1953). The data for the 3M coating, measured by the Metrology Division, NBS, are not necessarily typical, since the reflectance is very sensitive to coating techniques.

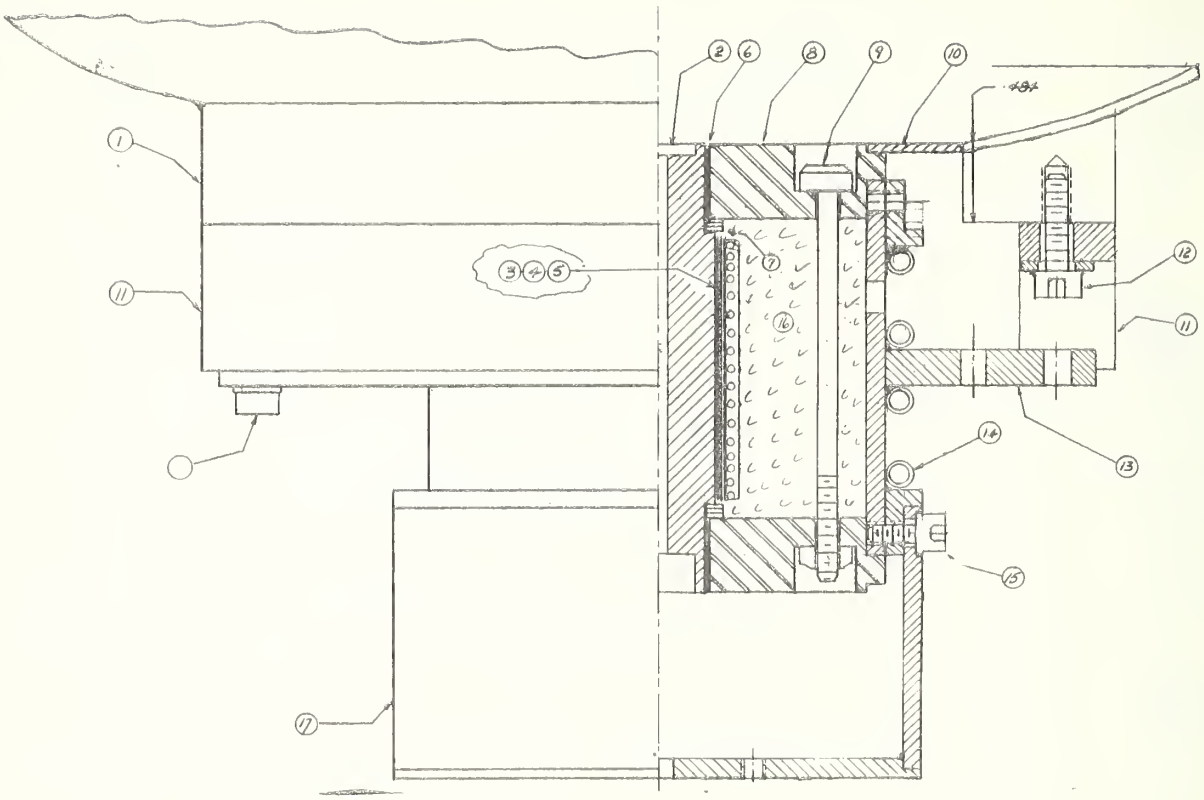

List & Description of Parts

1	Integrating sphere (14" OD) & 6" OD flange, flange outer flat surface is approx 1/2" below sphere at heater centerline
2	Heated silver core with cavities for 1/2" diameter specimens of .070" and .250" thicknesses, TC hole dia .099"
3,4,5	Three layers of GE asbestos paper, 5 ft 18 gauge (.050" D) nichrome wire @ .425 Ω/ft, aluminum phosphate cement coating
6,7	Mica spacers & washers, clearance at 6 is .030" clerance at 7 is 3/32"
8	End plate, 1/2" thick; transite coat with SiO_2-Na_2SiO_3
9	Tie down bolt, 1/8" dia nominal, 3 req'd at 120°, steel
10	Sphere wall filler disc, .065 thick, aluminum, coat with SiO_2, Na_2SiO_3
11	Alignment boss, aluminum
12	Cap screw 10-32, 3 req'd @ 120° with washer
13	Body assembly, brass
14	Cooling coils, 1/8" OD tubing
15	Cap screw 8-32, 3 req'd @ 120°
16	Insulation, Fiberfrax
17	Lower cap & cover, brass

Figure 3. Specimen heater designed to heat 1/2" diameter specimens to 800°K. Specimens of metals (0.065 in. thick) and dielectrics (0.25" thick) can be accommodated in the cavities at the respective ends of the silver core.

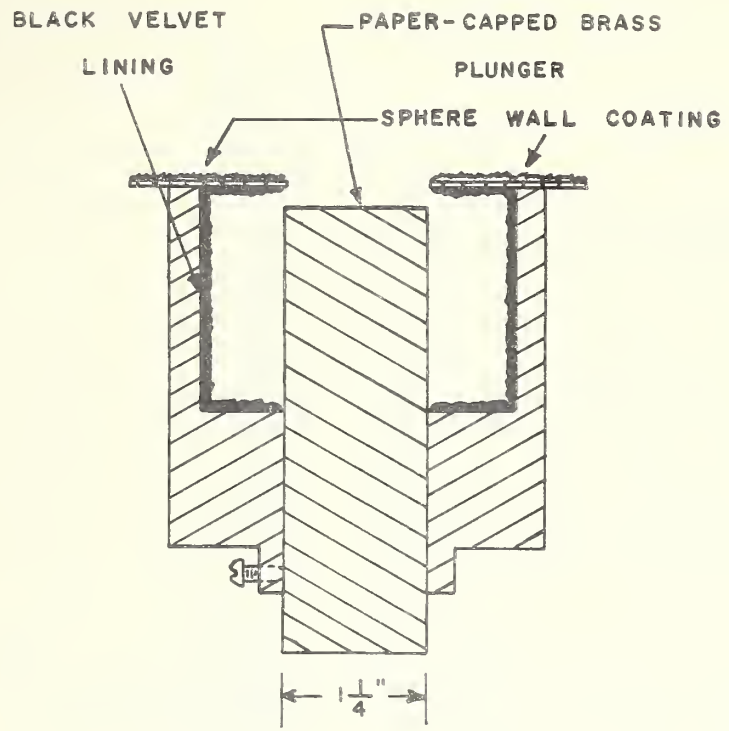

a) First reflection cavity. The base of the cavity is a diffuse reflector, but the walls are lined with black Velvet, so that only the first reflection from the base is permitted to escape from the cavity opening.

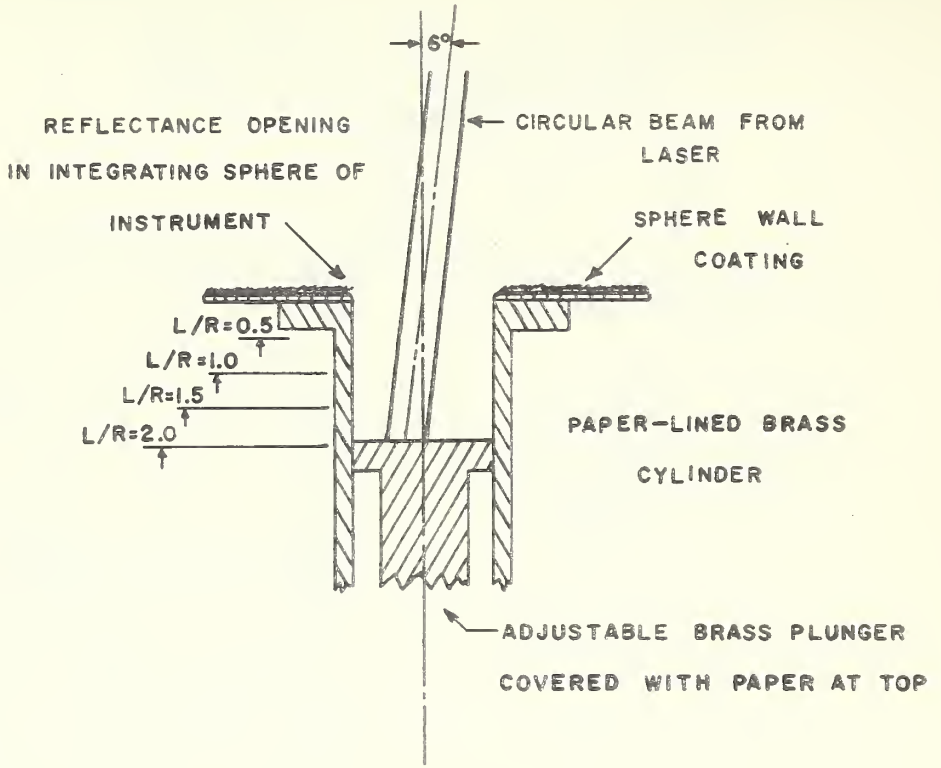

b) Lined cavity. Both base and walls of the cavity reflect diffusely. The movable plunger in each cavity permits the depth and radius (L/R) ratio to be varied from 0 to 2.0. 3M yellow Velvet paper was used as the diffusely reflecting surfaces.

Figure 4.

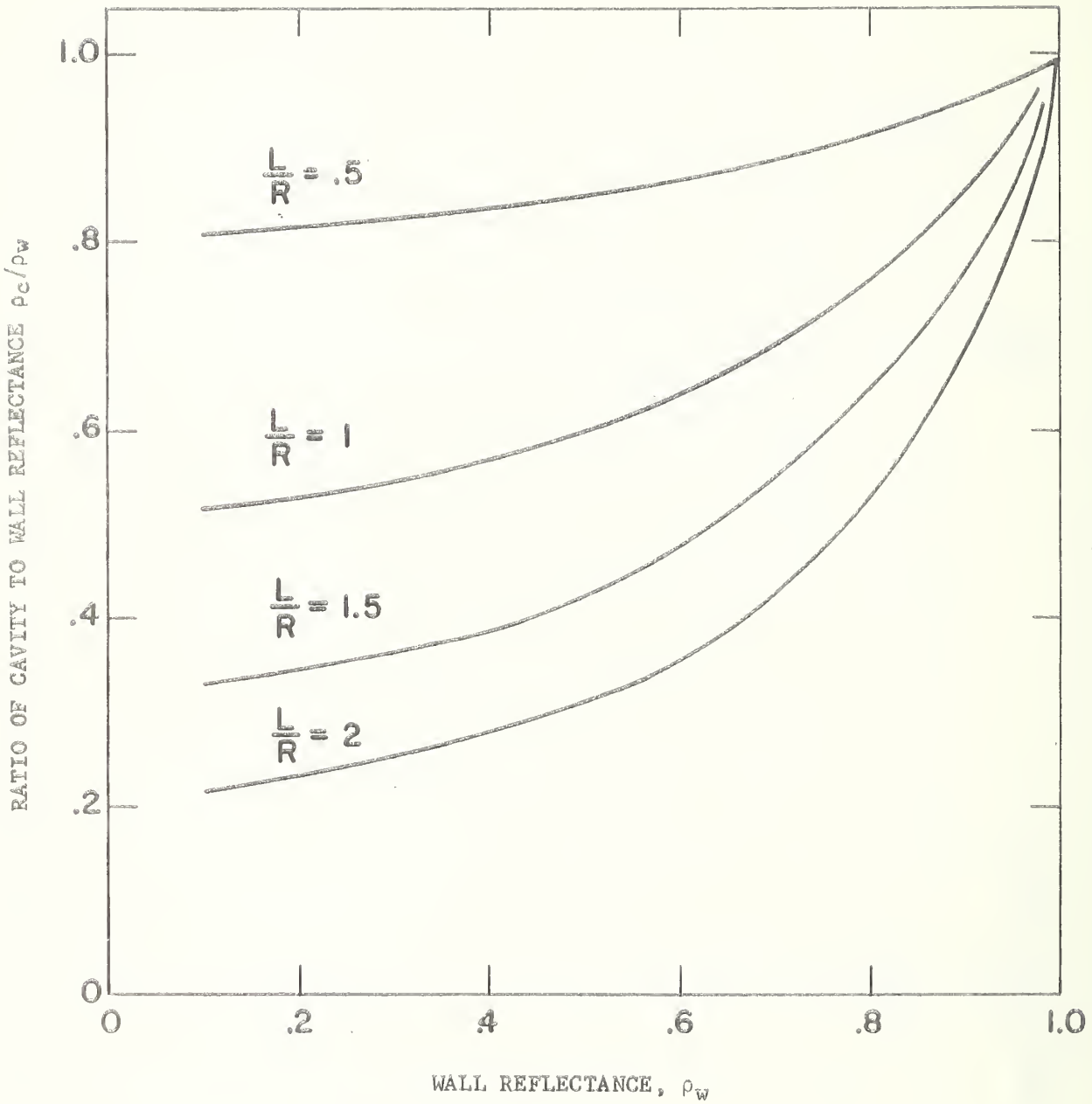

Figure 5. Ratio of cavity reflectance, ρ_c to wall reflectance, ρ_w, plotted as a function of depth-to-radius (L/R) ratio for different values of ρ_w, for center point illumination as computed by Equation 4.

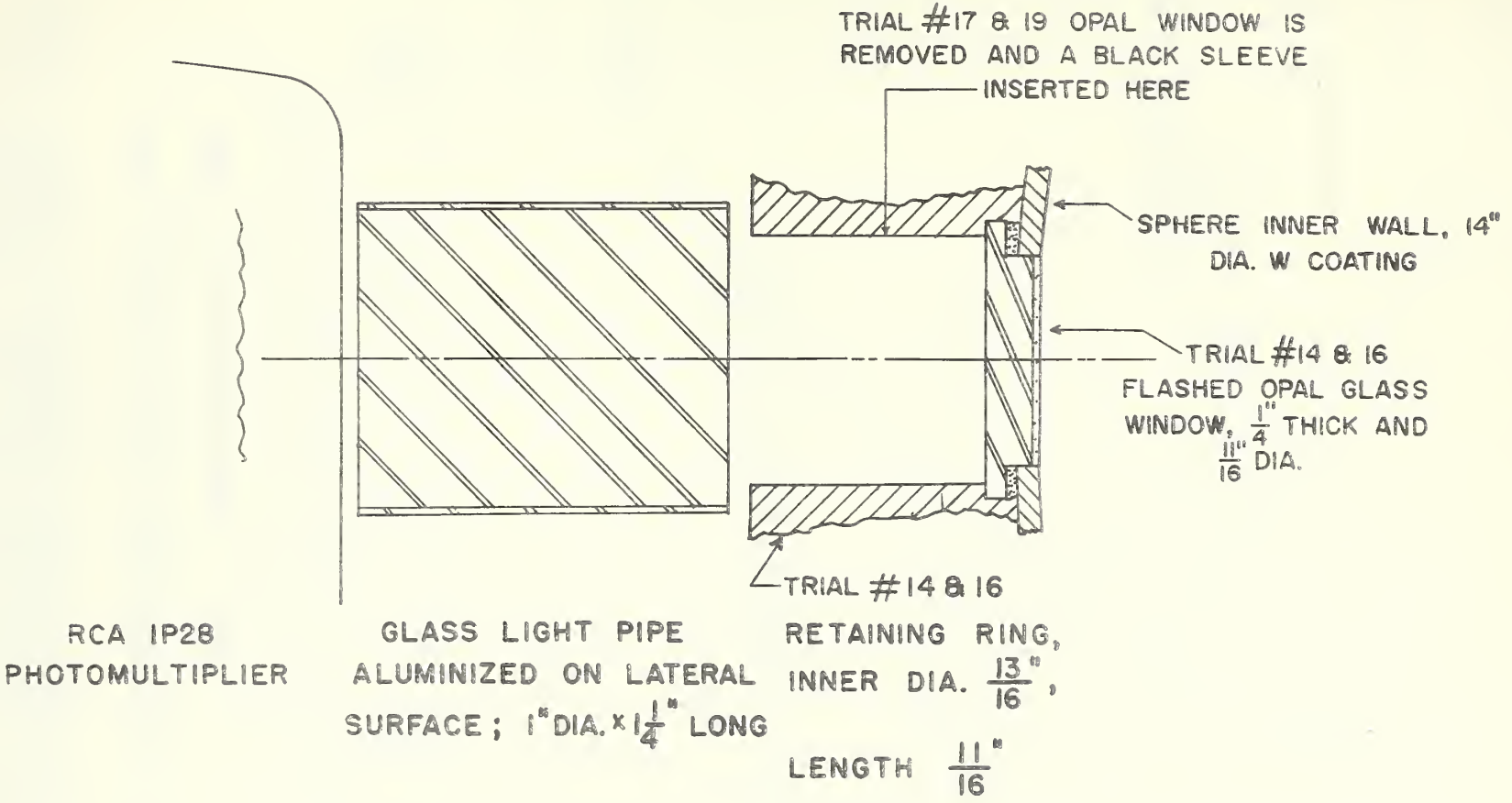

Figure 6. Sketch of detector mount and detector port on integrating sphere. With opal glass window in place the detector views the window. With window removed and black sleeve in place, detector views an area of the sphere wall diametrically opposite the detector port.

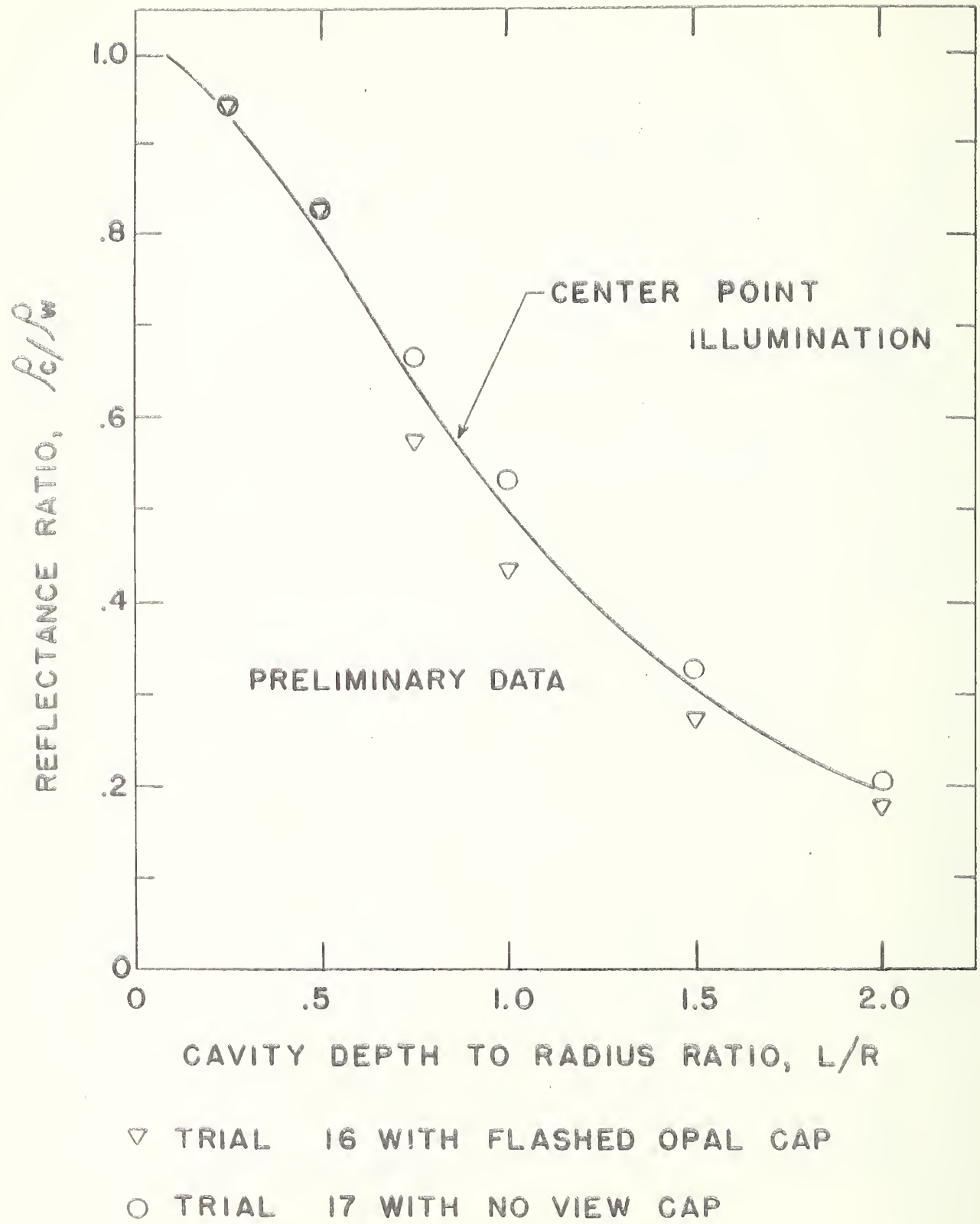

Figure 7. Ratios of reflectance of cavity to reflectance of bottom (ρ_c/ρ_w) as experimentally determined with the first reflection cavity, plotted as a function of depth-to-radius (L/R) ratio. Two different detector viewing configurations were used, as shown in Fig. 6. The solid curve is computed for center point illumination.

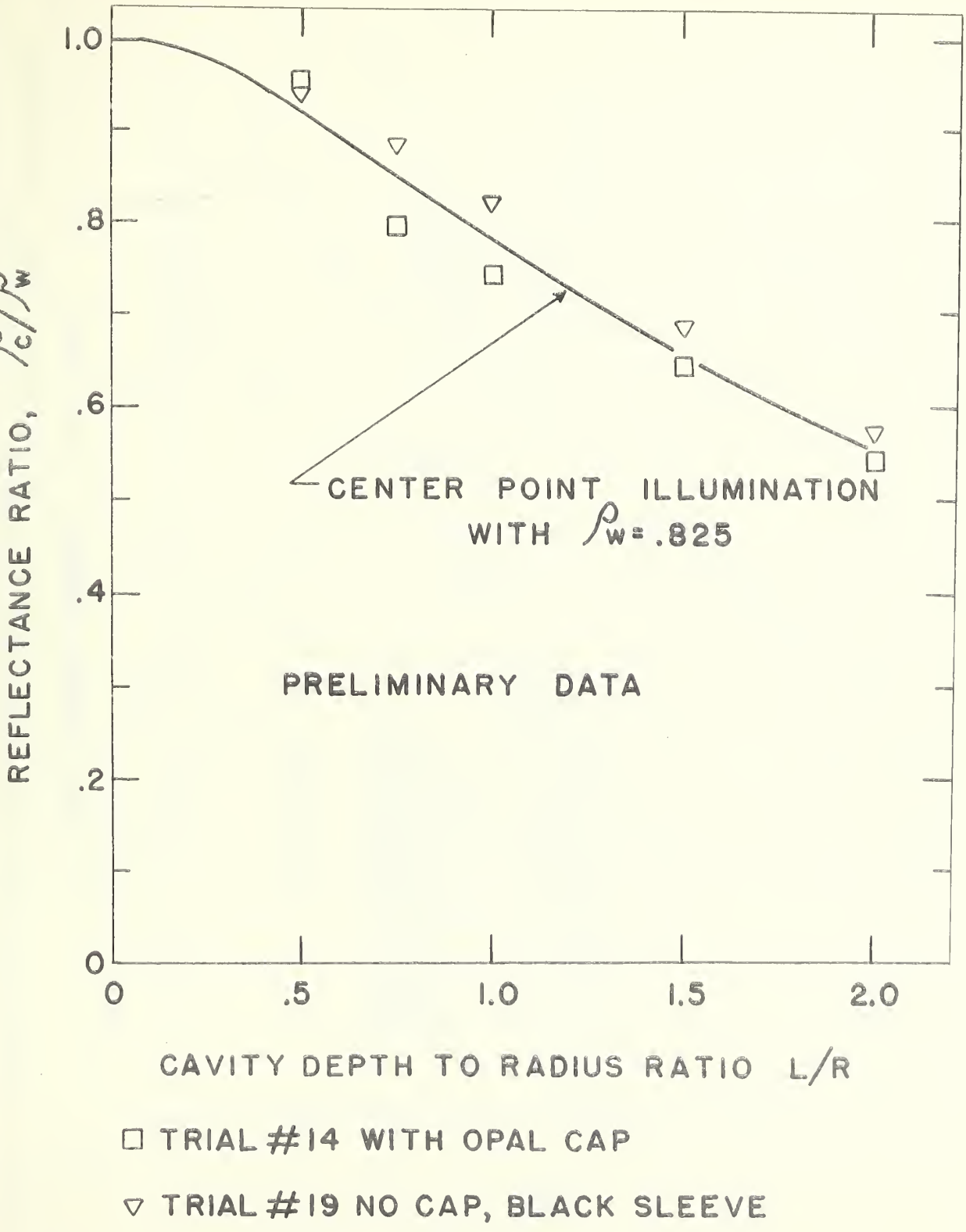

Figure 8. Ratios of reflectance of cavity to reflectance of walls (ρ_c/ρ_w) as experimentally determined with the lined cavity plotted as a function of depth-to-radius(L/R) ratio. Two different detector viewing configurations were used, as shown in Fig. 6. The solid curve is computed for center point illumination.

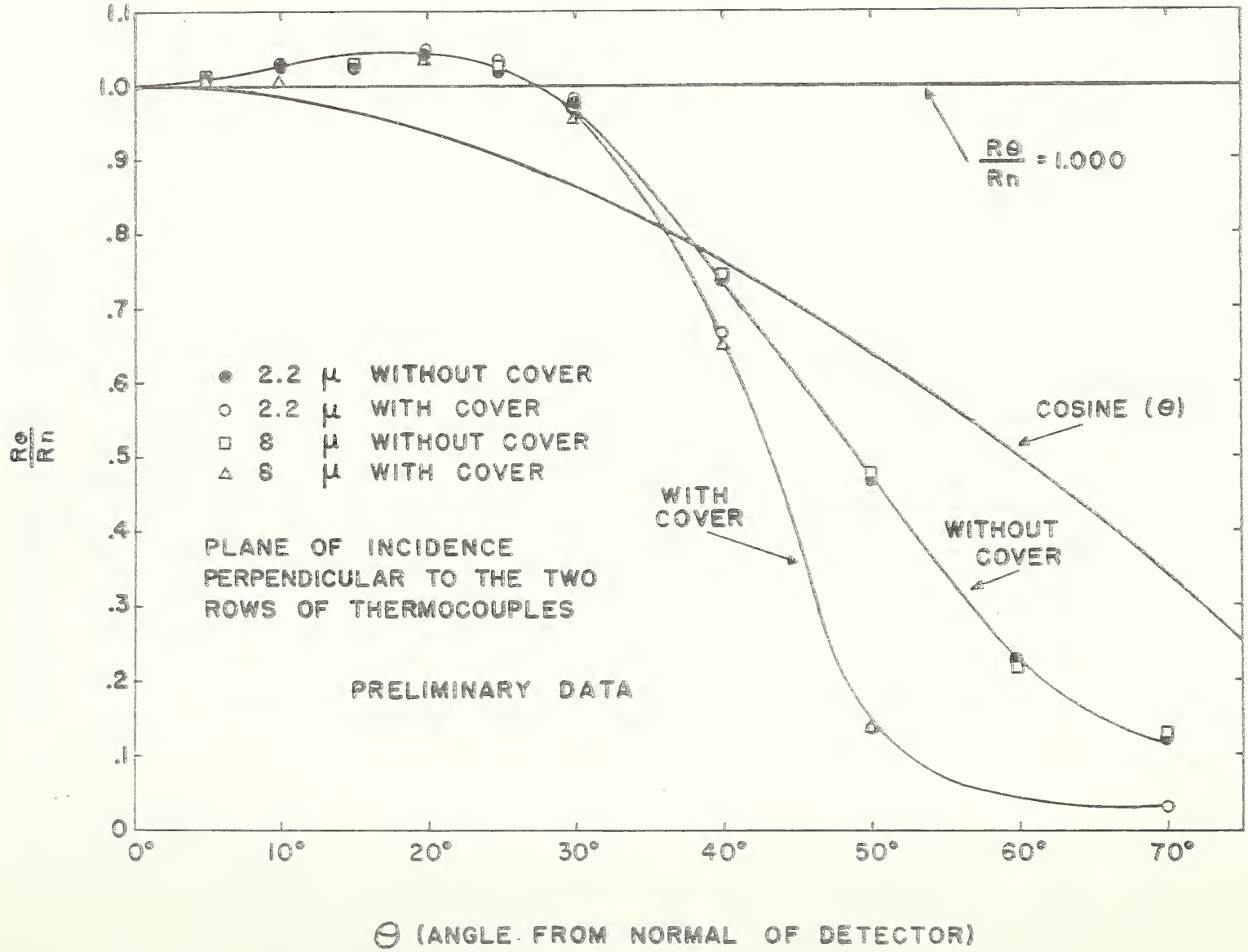

Figure 9. Angular sensitivity of Reeder Thermopile at 2.2 microns and 8 microns, with and without a detector mount cover, taken across the two rows of thermocouples.

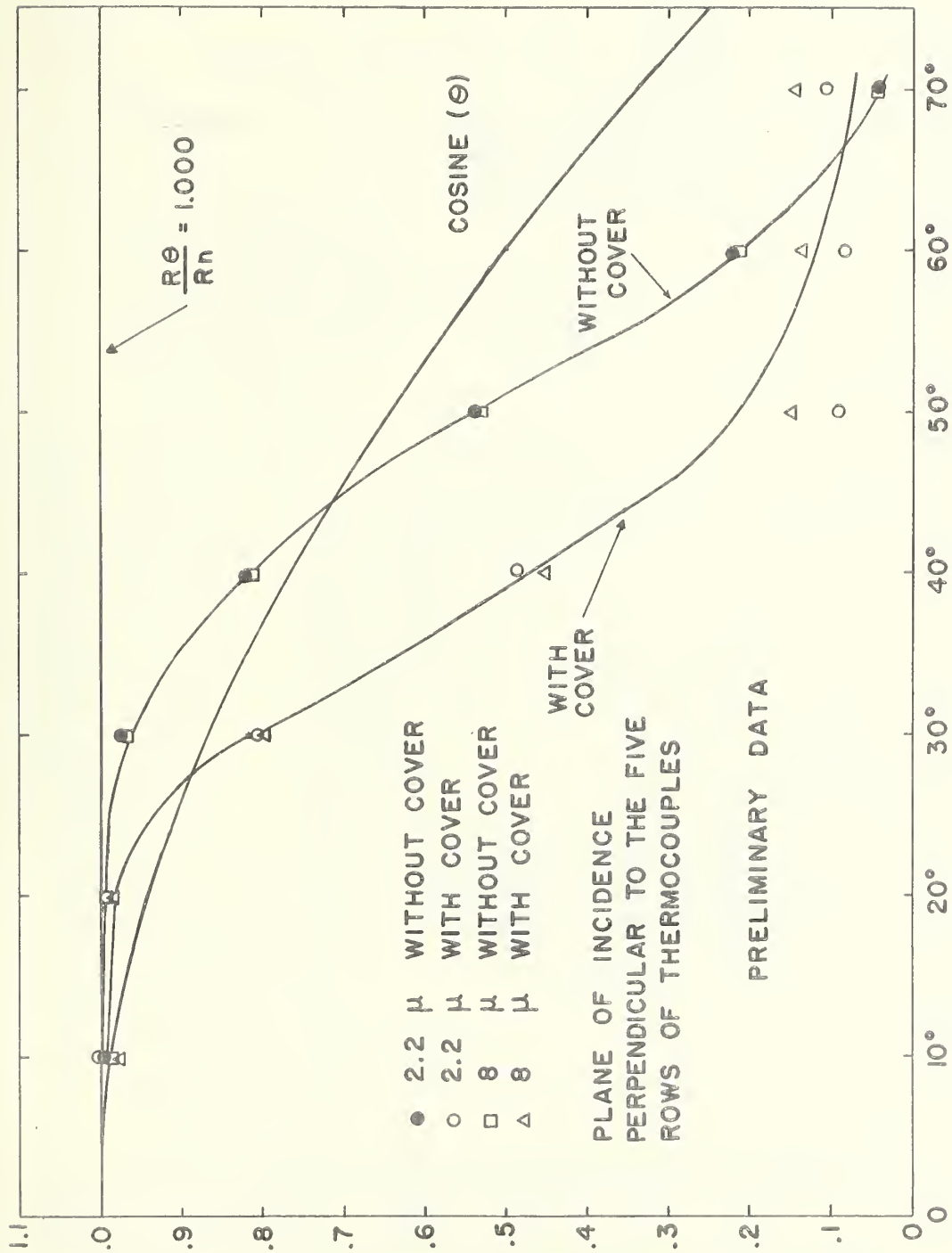

Figure 10. Angular sensitivity of Reeder Thermopile at 2.2 microns and at 8 microns, with and without detector mount cover, taken across the five rows of thermocouples.

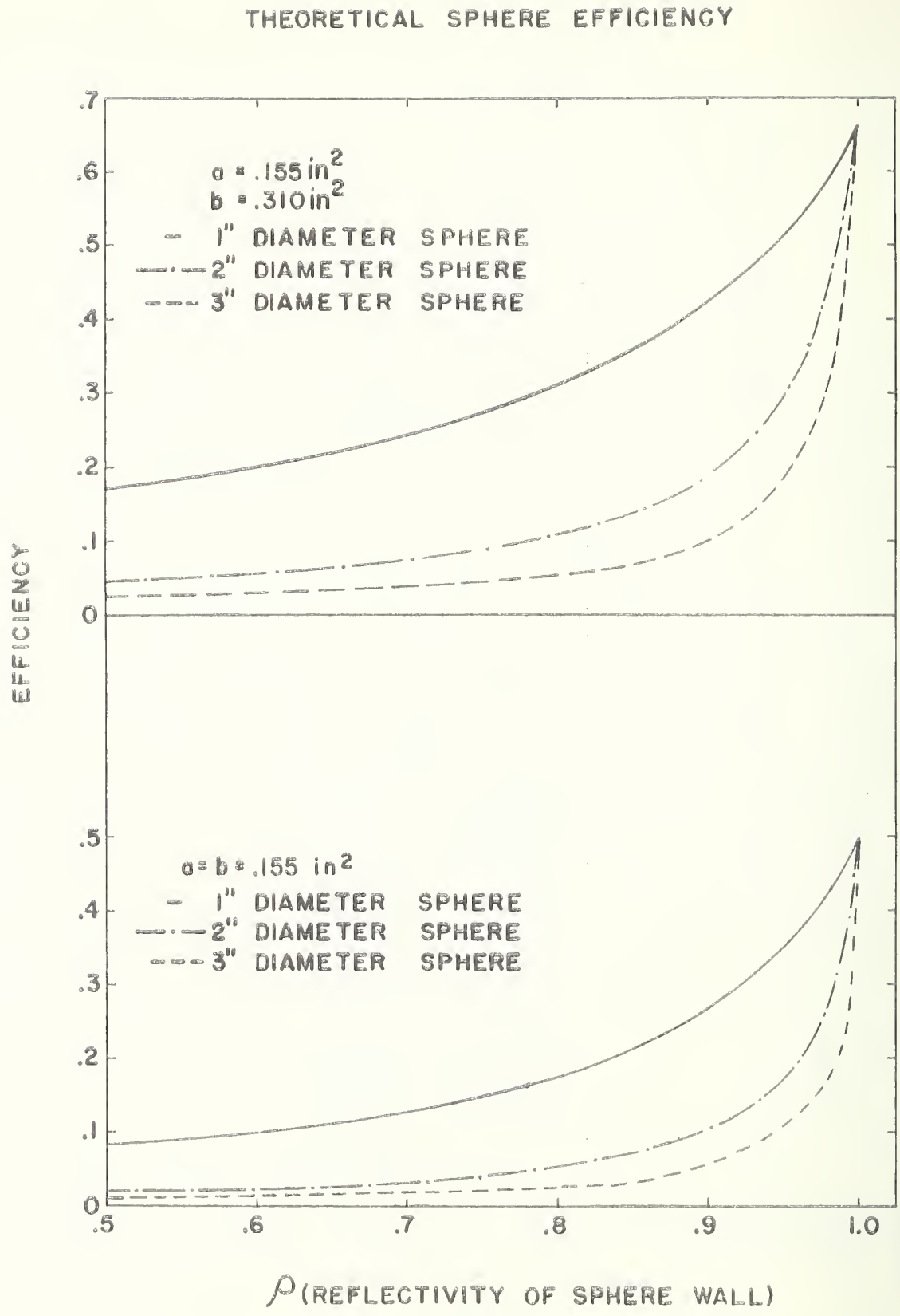

Figure 11. Efficiency of an integrating sphere as a function of diffuse reflectance of the walls for different diameter spheres, and different size entrance and exit ports.

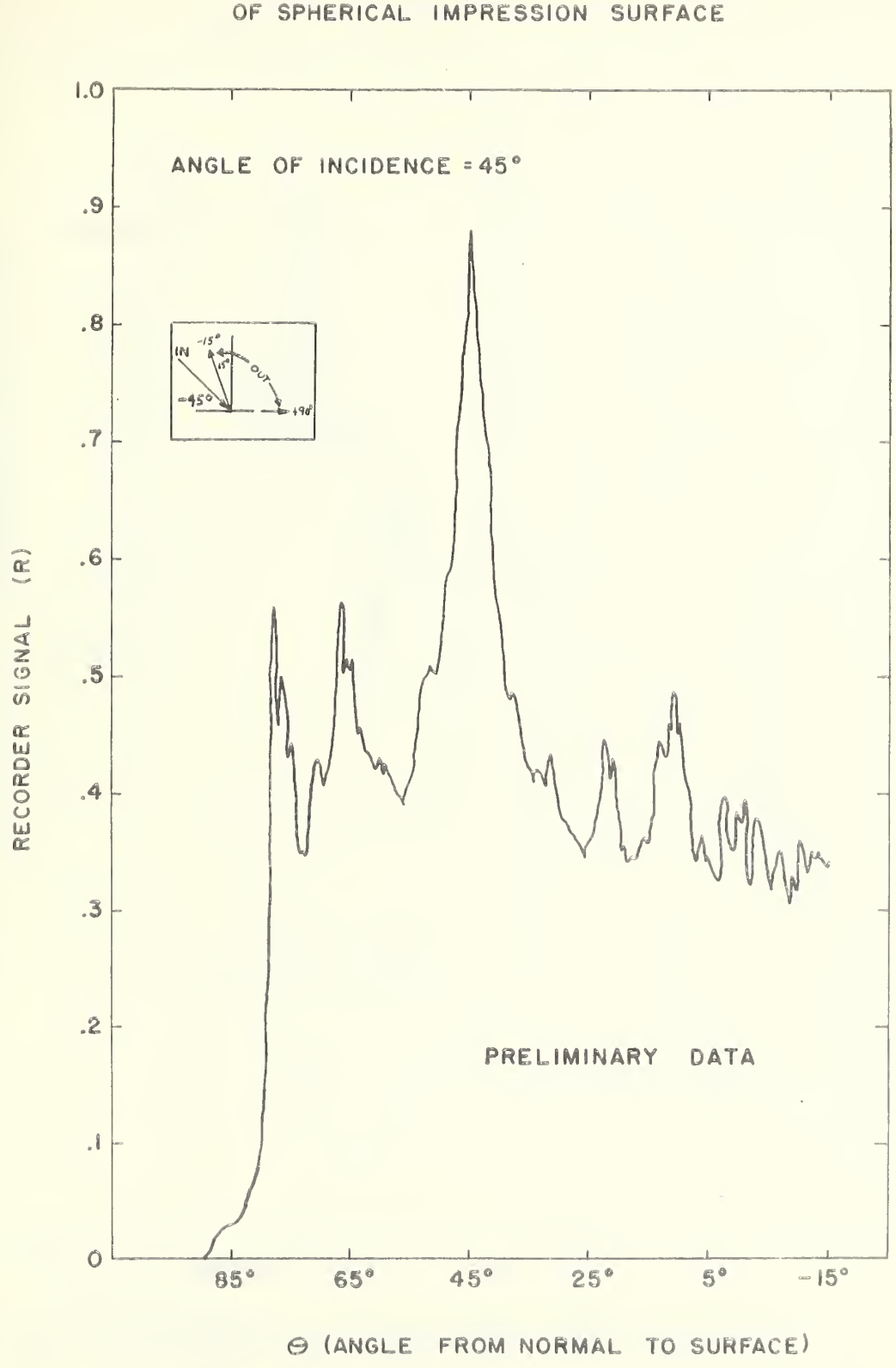

Figure 12. Goniophotometric data of spherical impression surface for 45° incidence angle.

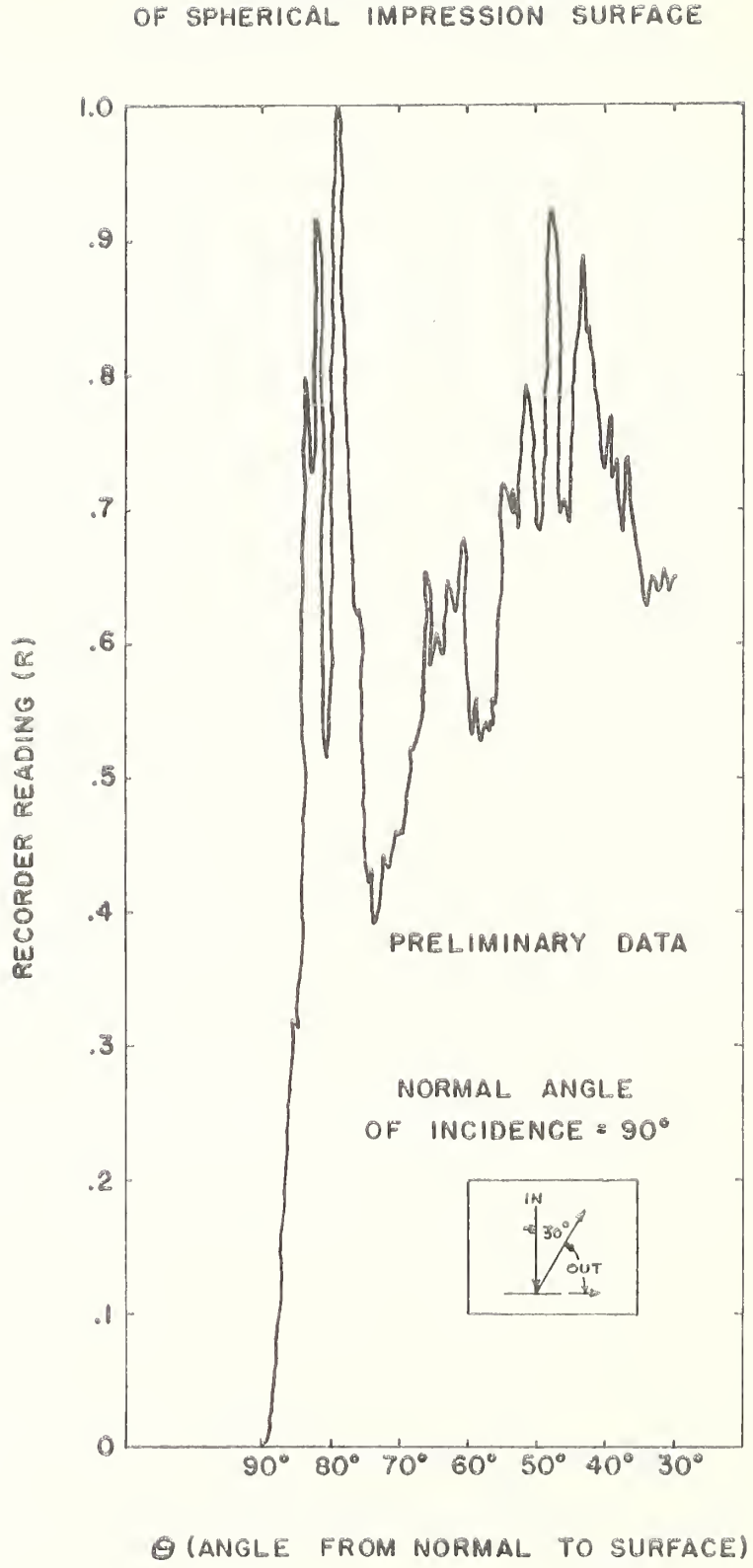

Figure 13. Goniophotometric data of spherical impression surface for normal incidence.

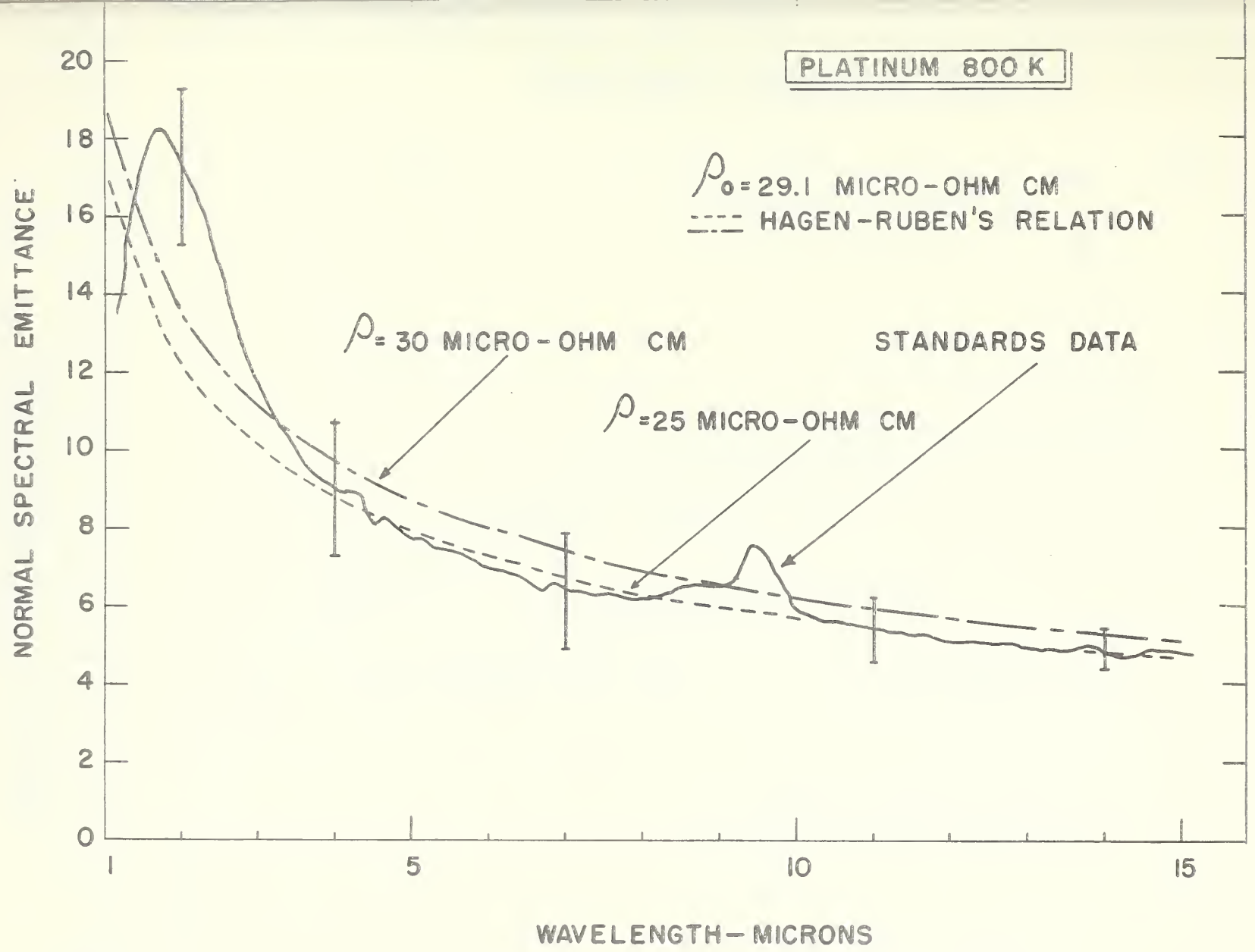

Figure 14a . Normal spectral emittance of platinum working standards at 800°K, compared to values computed from the Hagen-Rubens equation. The resistivity of platinum in micro-ohm centimeters is 29.1 at 800°K.

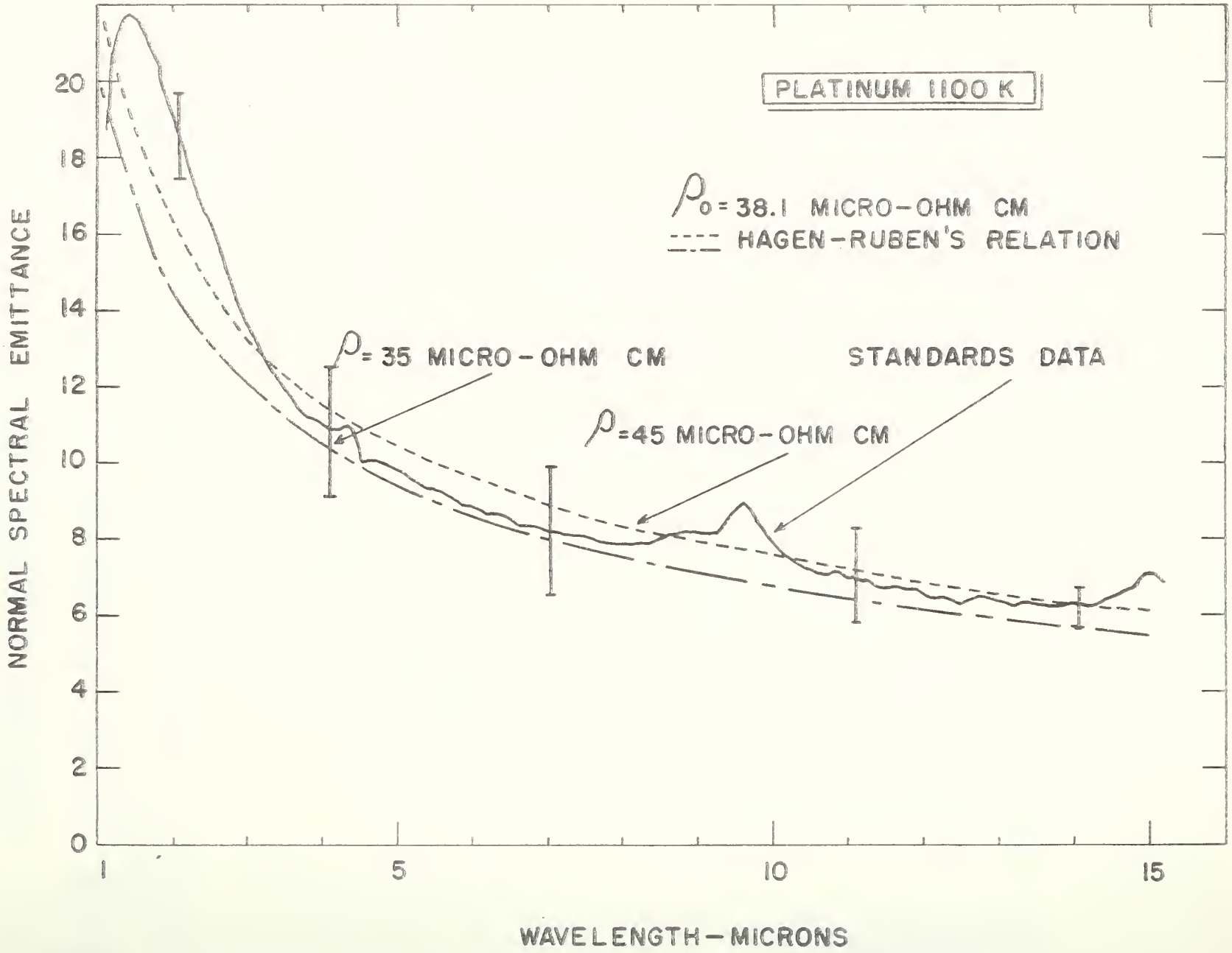

Figure 14b. Normal spectral emittance of platinum working standards at 1100°K, compared to values computed from the Hagen-Rubens equation. The resistivity of platinum in micro-ohm centimeters is 38.1 at 1100°K.

meters is 38.1 at 1100°K.

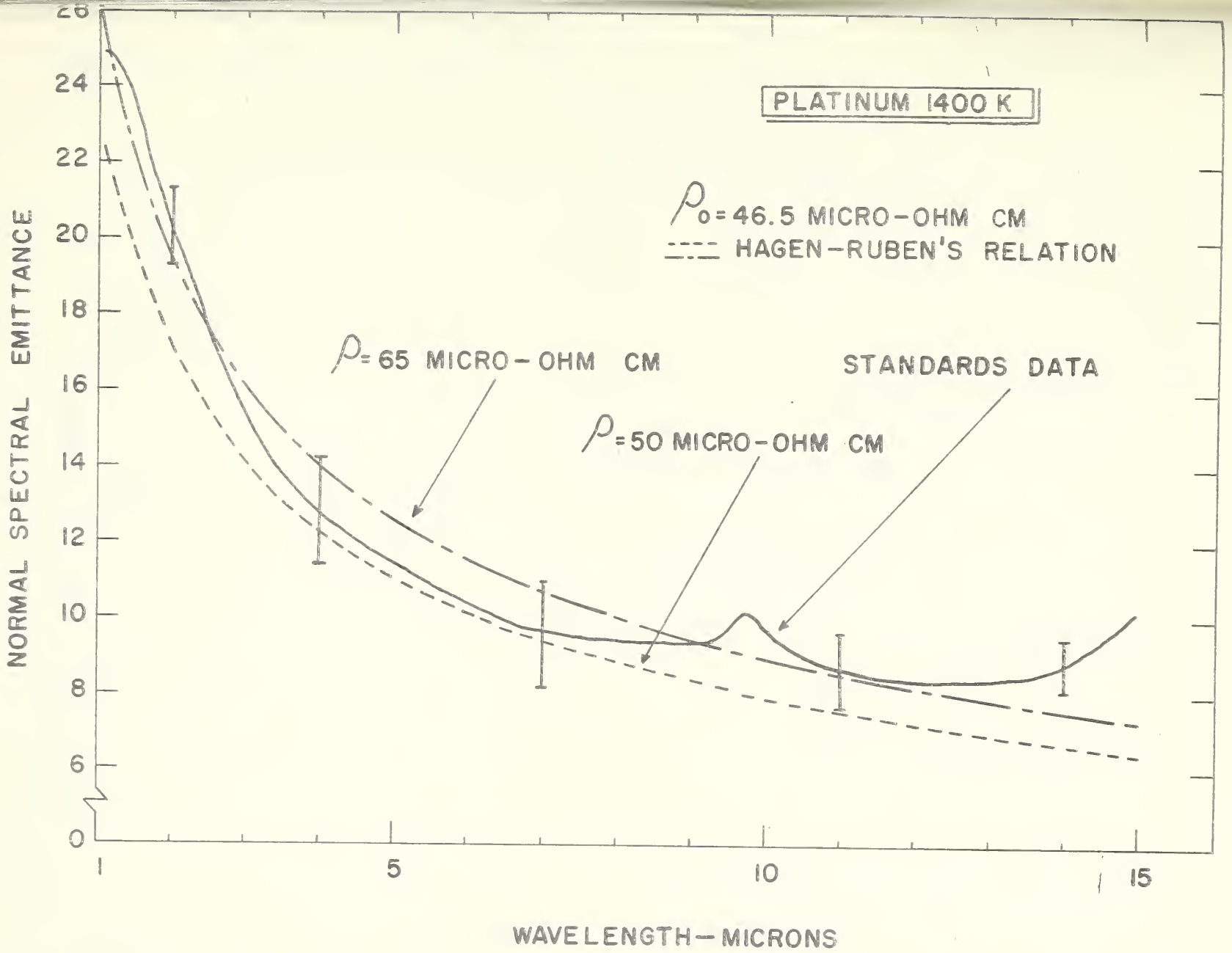

Figure 14c. Normal spectral emittance of platinum working standards at 1400°K, compared to values computed from the Hagen-Rubens equation. The resistivity of platinum in micro-ohm centimeters is 46.5 at 1400°K.

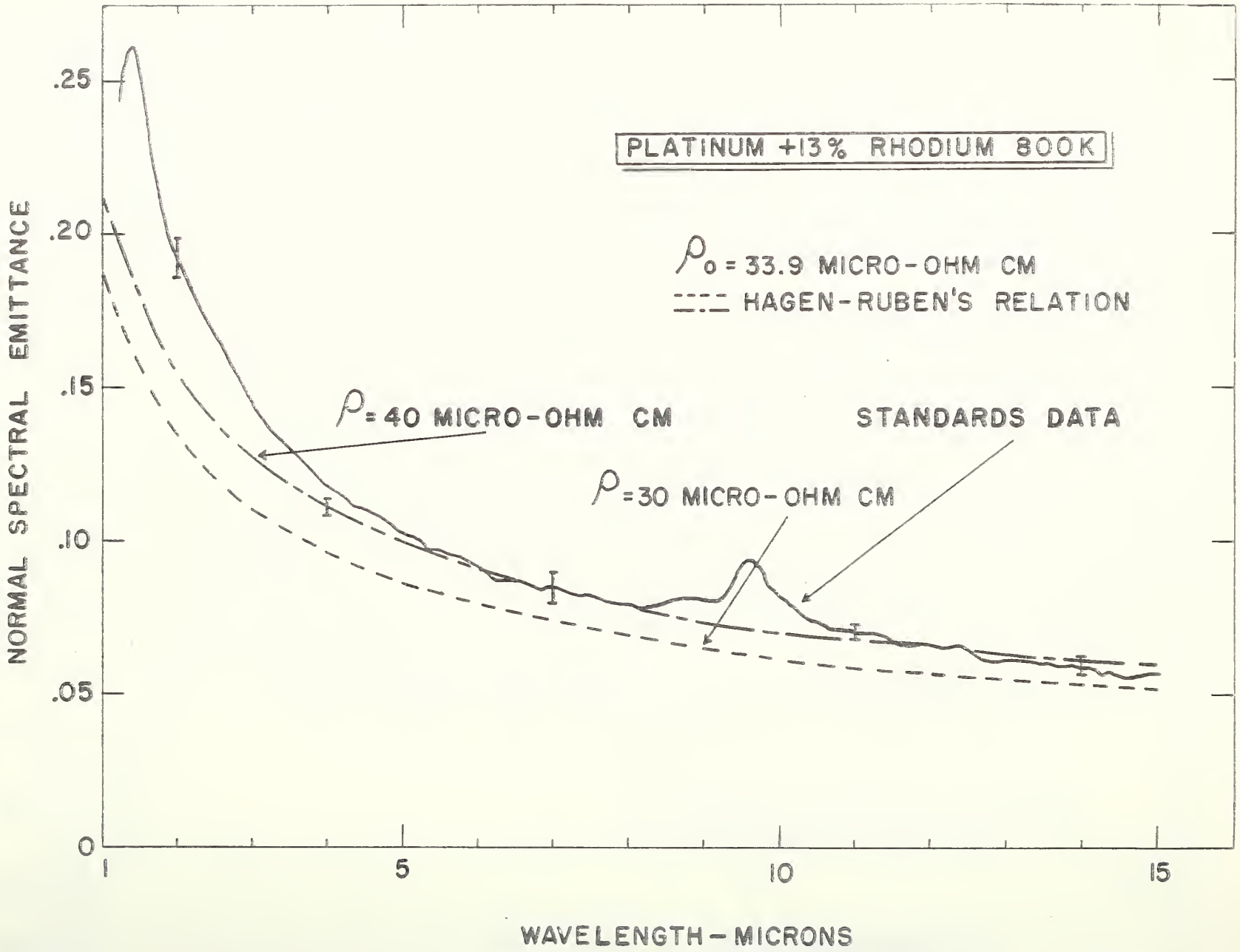

Figure 15a. Normal spectral emittance of platinum-13% rhodium alloy at 800°K, compared to values computed from the Hagen-Rubens equation. The resistivity of platinum-13% rhodium alloy in micro-ohm centimeteres is 33.9 at 800°K.

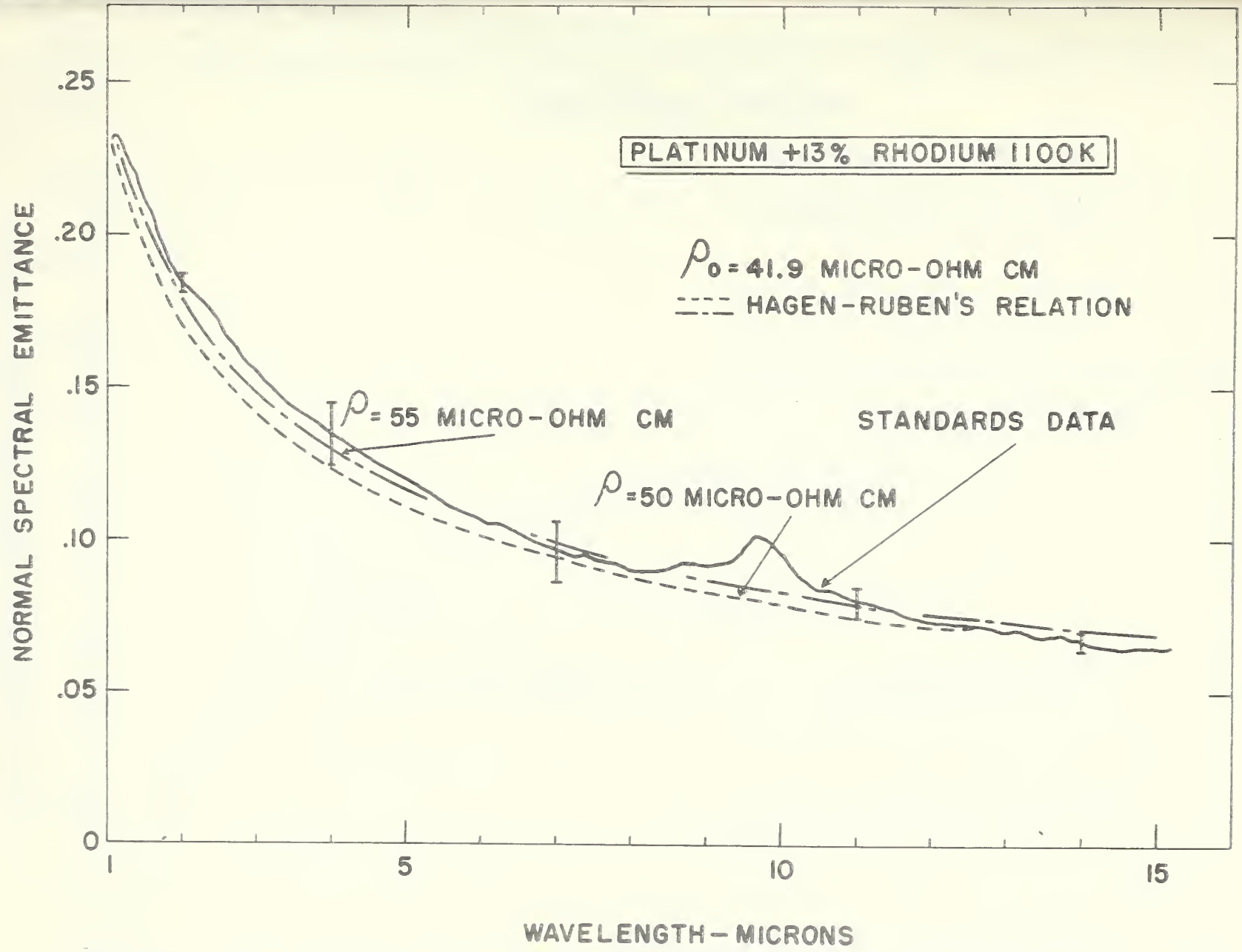

Figure 15b. Normal spectral emittance of platinum-13% rhodium alloy at 1100°K, compared to values computed from the Hagen-Rubens equation. The resistivity of platinum-13% rhodium alloy in micro-ohm centimeters is 41.9 at 1100°K.

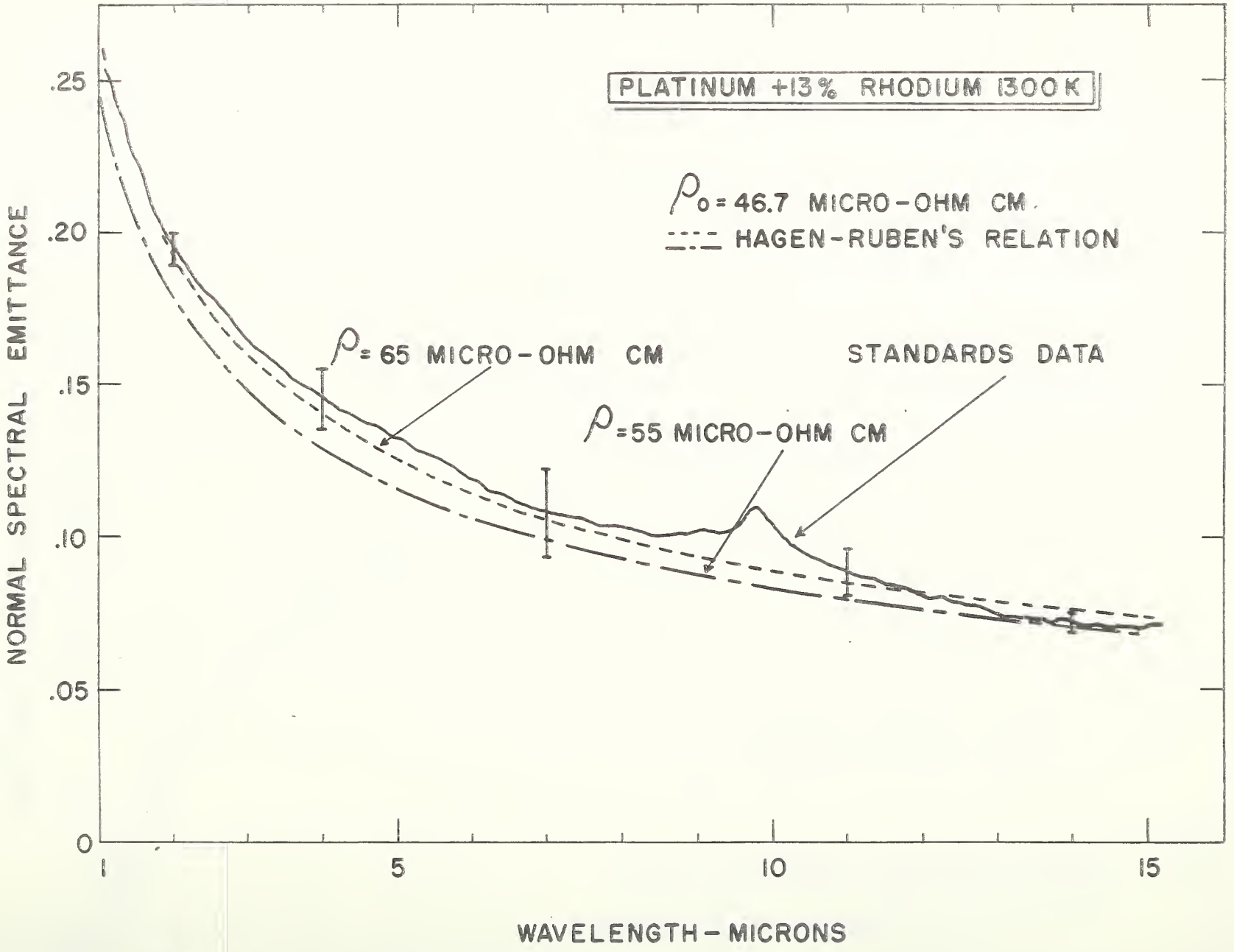

Figure 15c. Normal spectral emittance of platinum-13% rhodium alloy at 1300°K, compared to values computed from the Hagen-Rubens equation. The resistivity of platinum-13% rhodium alloy in micro-ohm centimeters is 46.7 at 1300°K.

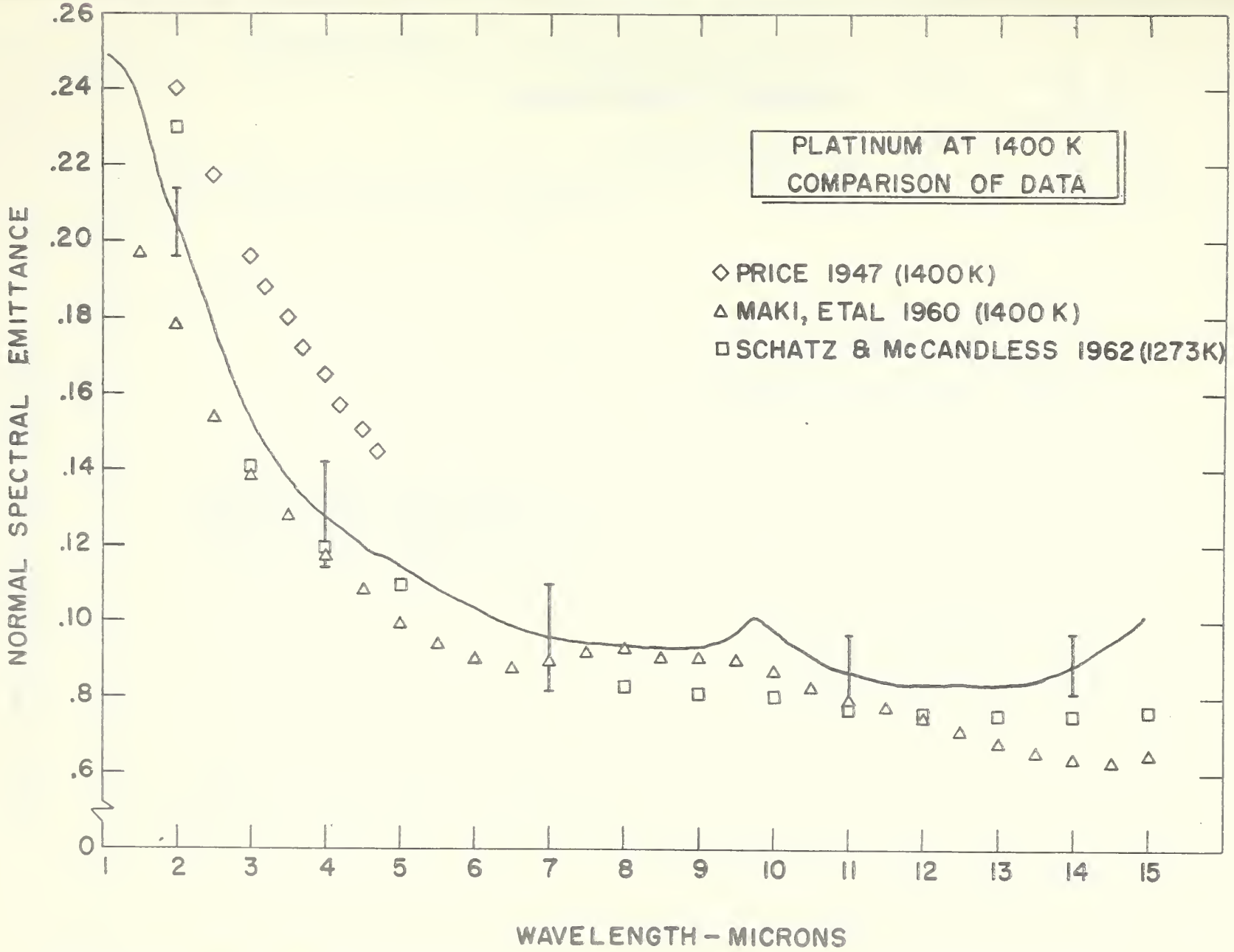

Figure 16. Normal spectral emittance of platinum at 1400°K, compared to literature values.

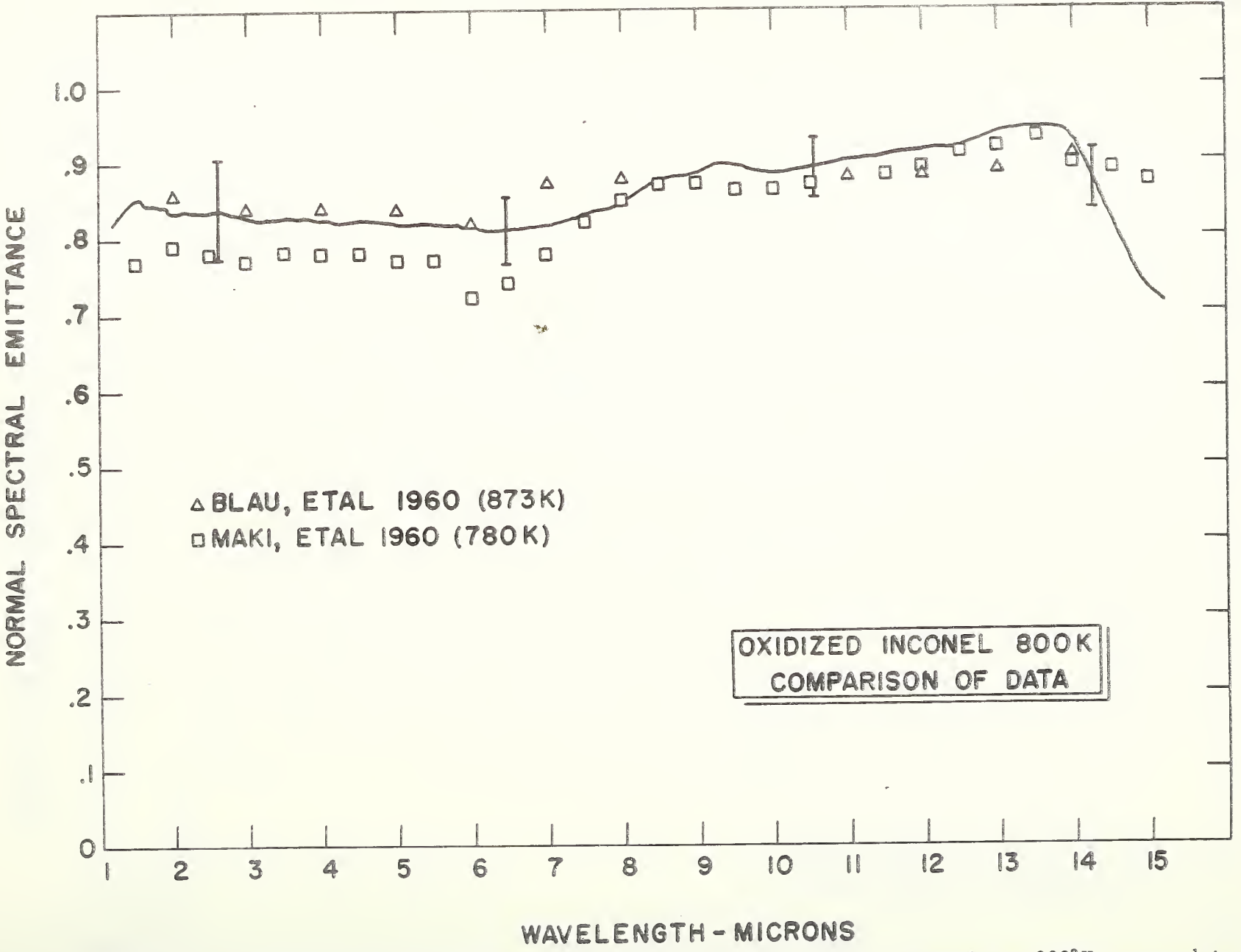

Figure 17a. Normal spectral emittance of oxidized Inconel working standards at 800°K compared to literature values.

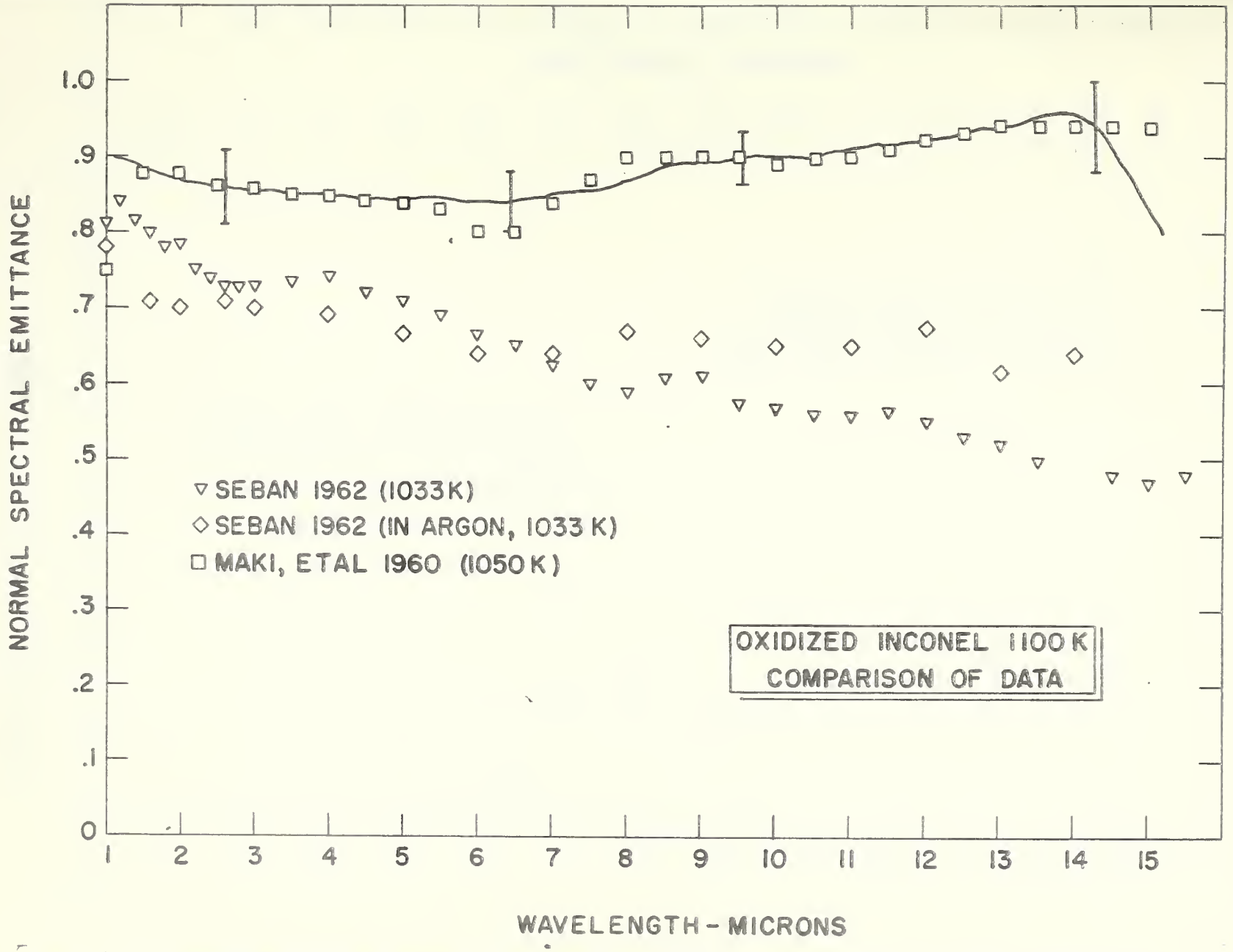

Figure 17b. Normal spectral emittance of oxidized Inconel working standards at 1100°K compared to literature values.

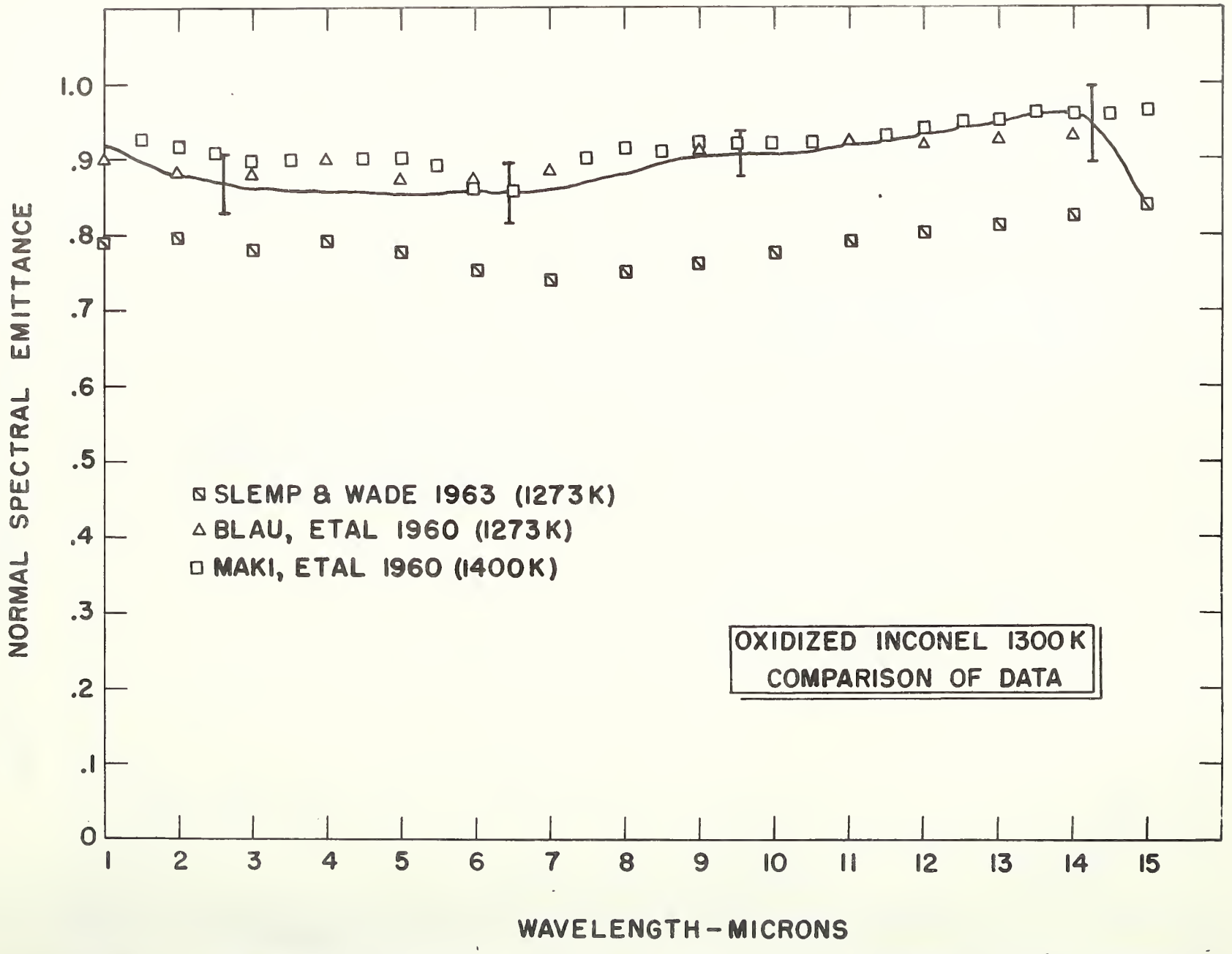

Figure 17c. Normal spectral emittance of oxidized Inconel working standards at 1300°K compared to literature values.

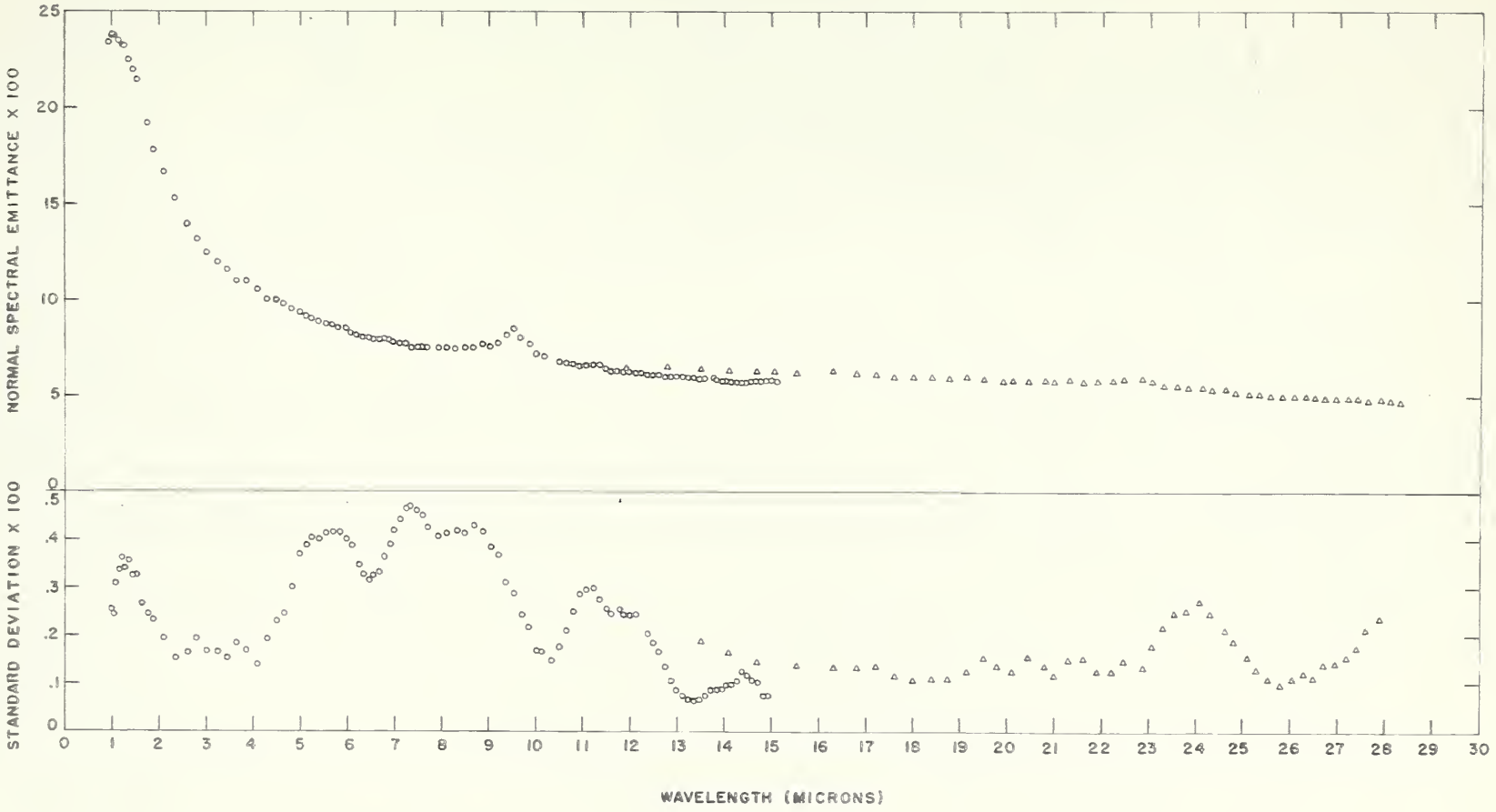

Figure 18. Top curve - normal spectral emittance of platinum working standard, measured with sodium chloride prism mounted in spectrometer, circles, and with cesium bromide prism mounted in spectrometer, triangles. The plotted points are averages of three determinations. Bottom curve - standard deviations of the average values plotted in the top curve.


DEPARTMENT OF COMMERCE
NATIONAL BUREAU OF STANDARDS